Research Square

Preprints are preliminary reports that have not undergone peer review.
They should not be considered conclusive, used to inform clinical practice,
or referenced by the media as validated information.

A Nash-Game Approach to Elliptic Cauchy Data Completion with Robust Error Bounds in Practical Noisy Regimes

Elyes Ahmed
SINTEF Digital
Saber Amdouni
saber.amdouni@enit.utm.tn
Tunis El Manar University
Amel Ben Abda
Tunis El Manar University

Research Article

Keywords: Cauchy problem, Data completion, Virtual control method, Nash equilibrium, Energy space approaches, Alternating minimization, Convergence analysis

Posted Date: August 6th, 2026

DOI: https://doi.org/10.21203/rs.3.rs-10527599/v1

License: This work is licensed under a Creative Commons Attribution 4.0 International License.
Read Full License

Additional Declarations: No competing interests reported.

A Nash-Game Approach to Elliptic Cauchy Data Completion with Robust Error Bounds in Practical Noisy Regimes

Elyes Ahmed*, Saber Amdouni†, and Amel Ben Abda†

July 31, 2026

Abstract

This paper presents a Nash game formulation for solving the ill-posed Cauchy problem associated with Laplace's equation. The data completion task is recast as a two-player static game, where each player controls a virtual Dirichlet condition on the inaccessible boundary. The first player minimizes a Neumann gap functional, while the second minimizes a Dirichlet gap functional, with both objectives coupled through a multiplier-based coupling term. A rigorous functional framework is developed in energy trace spaces. We prove the existence and uniqueness of the Nash equilibrium and show that, for compatible exact data, this equilibrium coincides with the missing trace of the exact solution of the Cauchy problem. In the presence of noisy measurements, Tikhonov regularization is incorporated into both players' cost functionals.

The main contribution of the paper is the derivation of explicit stability and error bound estimates for the regularized Nash equilibrium in a practical finite-noise regime. These estimates quantify the dependence of the reconstruction error on the noise level, the regularization parameter, and the coupling strength. In contrast with classical asymptotic convergence estimates, the proposed bounds are established uniformly for regularization parameters belonging to a fixed admissible interval $[\varepsilon, M]$, with $\varepsilon > 0$, and do not require additional spectral source-type assumptions on the exact missing data.

A conforming finite element discretization and an alternating minimization algorithm are then proposed. Numerical experiments on annular and half-annular domains confirm the robustness and accuracy of the method for nonzero noise levels and reduced-regularity configurations.

Keywords: Cauchy problem, Data completion, Virtual control method, Nash equilibrium, Energy space approaches, Alternating minimization, Convergence analysis.
Mathematics Subject Classification 65F22, 65N12, 65N15, 65N21, 65N22

Introduction

This paper addresses an inverse Cauchy problem using a gamified Nash equilibrium approach. Let $\Omega \subset \mathbb{R}^2$ be a bounded, connected Lipschitz domain with boundary $\partial\Omega = \Gamma$ partitioned into three non-overlapping parts: Γ_0, Γ_i, and Γ_c, such that

$$\Gamma = \overline{\Gamma_0 \cup \Gamma_i \cup \Gamma_c}, \quad \overline{\Gamma}_i \cap \overline{\Gamma}_c = \emptyset,$$

*SINTEF Digital, Forskningsveien 1, 0373 Oslo, Norway (elyes.ahmed@sintef.no)

†Laboratory For Mathematical And Numerical Modeling In Engineering Science, LAMSIN, LR99ES20, University of Tunis El Manar, National Engineering School of Tunis, Tunis, Tunisia (saber.amdouni@enit.utm.tn, amel.benabda@enit.utm.tn)

Corresponding author: Saber Amdouni

where Γ_i and Γ_c have positive measure (see Figure 1). The boundary Γ_i is inaccessible for measurements. We consider the Cauchy problem for Laplace's equation:

$$\begin{cases} \text{Given Cauchy data } (T, \phi) \text{ on } \Gamma_c, \text{ find } u : \Omega \to \mathbb{R} \text{ such that} \\ \quad -\Delta u = 0 \quad \text{in } \Omega, \quad u = T, \ \partial_n u = \phi \quad \text{on } \Gamma_c, \quad u = 0 \quad \text{on } \Gamma_0, \\ \text{where } \mathbf{n} \text{ denotes the unit outward normal vector to } \partial\Omega. \end{cases} \tag{1}$$

Note that recovering u is essentially equivalent to finding the unknown Dirichlet data $u_i := u|_{\Gamma_i}$ (and/or Neumann data $\partial_n u|_{\Gamma_i}$), assuming these boundary traces are well-defined. This Cauchy problem is ill-posed, as the solution lacks continuous dependence on the boundary data; consequently, small perturbations can lead to large, unbounded errors in the numerical solution [10].

This inverse problem finds important applications across various fields, notably in non-destructive testing [14] and electro-cardiology [15], among others. It has been studied extensively, from early foundations [28] to recent advances [44, 25, 11]; see [19, 9] for a comprehensive overview. In parallel, the theory of ill-posed problems was developed, with Hadamard's seminal analysis [28] clarifying the instability and non-uniqueness inherent to the Cauchy problem.

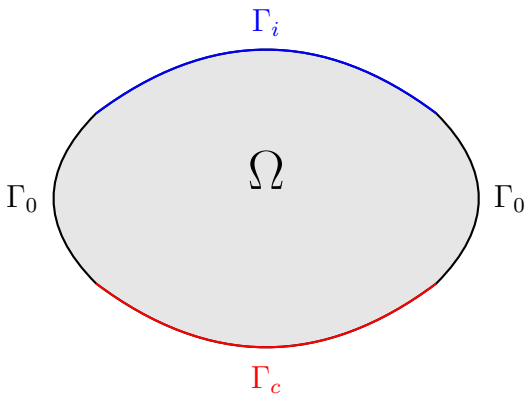


Figure 1: Domain geometry with boundary partitions

Several numerical approaches for reconstructing the missing boundary data, and subsequently solving the associated boundary value problem, can be broadly divided into direct, iterative, and Bayesian methods, where various regularization techniques are typically applied. Direct methods [11, 29, 8, 37] typically discretize an explicit operator mapping the unknown boundary data to the available measurements, often via boundary element [37, 22] or finite element techniques. The resulting ill-conditioned linear system is then stabilized using regularization methods such as Tikhonov regularization [48, 49, 46], Fading regularization [22, 51, 13, 1], projection techniques, or truncated singular value decomposition. In contrast, Bayesian methods [19, 20, 34, 30] treat the unknown as a random field, incorporating prior knowledge probabilistically to obtain a posterior distribution of possible solutions. However, the most widely used family for such problems is that of iterative methods, which generate a sequence of approximations where the regularization is intrinsically linked to the iteration process itself. This class includes Landweber-type iterations [19], conjugate gradient methods [2, 29], alternating procedures [35, 22, 18], and energy-error minimization [4, 5, 9].

A particularly interesting framework within this family reformulates the inverse problem as solving a coupled system of well-posed boundary value problems derived from the Kohn-Vogelius duplication method [33]. It is within this context that Nash game formulations [38, 42, 7] have emerged, casting data completion as a non-cooperative game between two players controlling Dirichlet and Neumann data. Building on this foundation, Habbal and Kallel [27] introduced

a static two-player Nash game for elliptic Cauchy problems, demonstrating how Neumann and Dirichlet data completion can be recast as interacting twin optimization problems. This idea was then extended to more complex inverse configurations including nonlinear elliptic equations [31], coupled data completion and conductivity reconstruction in cardiac electrophysiology [15], and detection of small inclusions in Stokes flow [40]. More recently, Roy and Pal [44] proposed a Nash-game framework for limited-data photoacoustic tomography, showing how Nash games can be integrated with modern optimization and machine-learning tools. A similar game-theoretic approach has also been successfully applied to domain decomposition methods [16, 32].

Classical regularization theory for ill-posed problems is usually formulated in an asymptotic setting, where both the noise level and the regularization parameter tend to zero. This framework is fundamental for proving convergence rates, but such rates generally rely on source-type or spectral regularity assumptions on the exact solution. In practical computations, however, the noise level is fixed and nonzero, and the regularization parameter cannot be chosen arbitrarily small without amplifying the noise. It is therefore important to complement the classical asymptotic analysis with robustness estimates that remain valid for admissible positive values of the regularization parameter. The present work follows this finite-noise perspective, inspired by the robustness analysis developed in [3] for an energy-space method applied to boundary data completion in linear elasticity. In that work, error bounds of the form

$$O\left(\frac{\delta}{\sqrt{\alpha}}+\sqrt{\alpha}\right)$$

were obtained uniformly for regularization parameters belonging to a fixed admissible interval, without imposing classical spectral source-type conditions. This motivates the extension of the same robustness-oriented philosophy to a new game-theoretic framework. More precisely, we introduce a Nash-game formulation for noisy ill-posed Cauchy problems governed by Laplace's equation. The method is based on a dual-control strategy: two independent virtual Dirichlet controls are introduced on the inaccessible boundary, each associated with a different auxiliary boundary value problem. One player controls the reconstruction through a Neumann gap functional, whereas the other controls it through a Dirichlet gap functional. The two players are coupled by a consistency term acting on the inaccessible boundary. The main contributions of this work are threefold. First, we establish a rigorous functional framework in energy trace spaces and prove the existence and uniqueness of a Nash equilibrium. For compatible exact data, this equilibrium coincides with the missing trace of the exact harmonic solution. Second, we introduce a Tikhonov-regularized Nash game for noisy measurements and derive explicit stability and error bounds. These estimates are valid in a practical finite-noise regime: the regularization parameter is kept in a fixed admissible interval $[\varepsilon, M]$, with $\varepsilon > 0$, and the constants are uniform with respect to α in this interval. Thus, the estimates quantify robustness for nonzero noise levels without imposing the classical spectral source conditions usually required to obtain comparable asymptotic Tikhonov rates. Third, we develop a conforming finite element discretization and an alternating minimization algorithm for the computation of the Nash equilibrium.

The paper is organized as follows. Section 1 introduces the virtual control formulation of the data completion problem and presents a novel static two-player Nash game framework. Within this setting, we establish the appropriate functional framework in energy trace spaces, define the players' cost functionals, and prove the existence and uniqueness of the Nash equilibrium. We also show that, under compatibility of the boundary data, the Nash equilibrium coincides with the exact solution of the Cauchy problem.

Section 2 is devoted to the stability analysis of the proposed Nash-game formulation in the presence of noisy measurements. A Tikhonov-regularized game is introduced, and explicit error bounds are derived for the regularized Nash equilibrium. These estimates quantify the combined

effects of the noise level δ, the regularization parameter α, and the coupling parameter γ. A particular emphasis is placed on the practical finite-noise regime $\alpha \in [\varepsilon, M]$, where the estimates remain uniform with respect to α and do not rely on classical source-type assumptions. The asymptotic case is recovered only when an additional parameter choice is imposed.

The analysis is then extended to the discrete setting in Section 3, where a finite element discretization of the continuous problem and the associated Nash game is presented. Stability and a priori error estimates are established for the discrete Nash equilibria, accounting for both discretization errors and data perturbations.

Having established the theoretical and discrete frameworks, Section 4 focuses on the numerical implementation of the proposed method. We describe the alternating minimization algorithm used to compute the Nash equilibrium, the finite element solution of the state and adjoint problems, and practical considerations related to parameter selection and computational efficiency.

Finally, Section 5 presents a series of numerical experiments that validate the theoretical findings. These results illustrate the accuracy, robustness, and convergence properties of the method under various noise levels and geometrical configurations. The paper ends with concluding remarks emphasizing the robustness of the method in finite-noise regimes and discussing possible extensions to more general elliptic systems and uncertainty-aware formulations.

1 Gamified Data Completion via Nash Equilibrium

1.1 Virtual Control Formulation

We begin by introducing the functional framework for the Cauchy problem (1). For boundary parts $\Gamma_k \subset \Gamma$ ($k \in \{i, c\}$), we employ the trace spaces from [47]:

$$H^{\frac{1}{2}}(\Gamma_k) = \left\{ v = \tilde{v}|_{\Gamma_k} : \tilde{v} \in H^{\frac{1}{2}}(\Gamma) \right\}, \quad \widehat{H}^{\frac{1}{2}}(\Gamma_k) = \left\{ v = \tilde{v}|_{\Gamma_k} : \tilde{v} \in H^{\frac{1}{2}}(\Gamma),\ \tilde{v}|_{\Gamma \setminus \overline{\Gamma}_k} = 0 \right\}.$$

The Lions-Magenes spaces $\widehat{H}^{\frac{1}{2}}(\Gamma_k)$ [36] and their duals $\widehat{H}^{-\frac{1}{2}}(\Gamma_k)$ are equipped with the energy norms:

$$\|w\|^2_{\widehat{H}^{\frac{1}{2}}(\Gamma)} = \langle S_{DN} w, w \rangle_\Gamma, \quad \|\lambda\|^2_{\widehat{H}^{-\frac{1}{2}}(\Gamma)} = \langle \lambda, S_{ND} \lambda \rangle_\Gamma,$$

defined via the Dirichlet-to-Neumann operator S_{DN} and its inverse S_{ND} [45, 41].

The core of our approach is a dual-control strategy that generalizes the standard Dirichlet-to-Neumann method [27]. We introduce independent virtual controls η_D and η_N on Γ_i, each governing different physical aspects through two complementary problems:

$$\begin{cases} \text{Find } u_D \in H^1(\Omega) \text{ such that} \\ -\Delta u_D = 0 \text{ in } \Omega, \quad u_D|_{\Gamma_0} = 0, \\ u_D|_{\Gamma_c} = T, \quad u_D|_{\Gamma_i} = \eta_D. \end{cases} \tag{P_D}$$

$$\begin{cases} \text{Find } u_N \in H^1(\Omega) \text{ such that} \\ -\Delta u_N = 0 \text{ in } \Omega, \quad u_N|_{\Gamma_0} = 0, \\ \partial_n u_N|_{\Gamma_c} = \phi, \quad u_N|_{\Gamma_i} = \eta_N. \end{cases} \tag{P_N}$$

A key advantage of keeping η_D and η_N independent is twofold: it introduces robustness against data noise by confining errors to their respective boundary types, and it offers built-in regularization via variable isolation. Moreover, interpreting S_{DN} and S_{ND} as solution operators (with a slight abuse of notation), the required controls must also fulfill the interfacial consistency conditions:

$$\begin{cases} \text{Given } T \text{ and } \phi, \text{ find } (\eta_D, \eta_N) \in (\widehat{H}^{\frac{1}{2}}(\Gamma_i))^2 \text{ such that:} \\ \quad S_{ND}(\phi; \eta_N) = u_N|_{\Gamma_c}, \text{ and } S_{DN}(T; \eta_D) = \partial_n u_D|_{\Gamma_c}, \\ \text{with } u_D \text{ and } u_N \text{ defined by } (\mathrm{P}_D) \text{ and } (\mathrm{P}_N). \end{cases} \tag{2}$$

This dual structure invites a game-theoretic interpretation: two players, selecting independent strategies η_D and η_N, must coordinate to produce consistent solutions on the interface Γ_c. The framework is reminiscent of gamified Domain Decomposition (DD) methods [16] but with a key distinction: it operates on a single domain Ω using *twin systems* that compete and cooperate via virtual controls on an internal interface Γ_i, rather than across multiple physical subdomains.

To implement this gamified approach, we formulate the hybrid variational problems. For the Dirichlet problem (P_D) with $g_{D,i} = \eta_D$, $g_{D,c} = T$, $g_{D,0} = 0$:

$$\begin{cases} \displaystyle\int_\Omega \nabla u_D \cdot \nabla v_D d\Omega - \sum_{k\in\{i,c,0\}} \langle \lambda_D^k, v_D\rangle_{\Gamma_k} = 0, \\ -\langle \mu_D^k, u_D - g_{D,k}\rangle_{\Gamma_k} = 0, \quad k \in \{i,c,0\}. \end{cases} \tag{3}$$

For the Neumann problem (P_N) with $g_{N,i} = \eta_N$, $g_{N,0} = 0$:

$$\begin{cases} \displaystyle\int_\Omega \nabla u_N \cdot \nabla v_N d\Omega - \sum_{k\in\{i,0\}} \langle \lambda_N^k, v_N\rangle_{\Gamma_k} = \langle \phi, v_N\rangle_{\Gamma_c}, \\ -\langle \mu_N^k, u_N - g_{N,k}\rangle_{\Gamma_k} = 0, \quad k \in \{i,0\}. \end{cases} \tag{4}$$

These formulations admit unique solutions with $\lambda_D^c = \partial_n u_D|_{\Gamma_c}$, $\lambda_D^i = \partial_n u_D|_{\Gamma_i}$, and $\lambda_N^i = \partial_n u_N|_{\Gamma_i}$.

1.2 Cost Functionals and Game Strategy

We now cast the data completion problem as a two-player cooperative Nash game. The players, associated with the controls $(\eta_D, \eta_N) \in (\widehat{H}^{\frac{1}{2}}(\Gamma_i))^2$, cooperate to minimize their respective misfit functionals derived from (2):

$$H_D(\eta_D,\eta_N) = \frac{1}{2}\|\lambda_D^c(T,\eta_D) - \phi\|^2_{\widehat{H}^{-\frac{1}{2}}(\Gamma_c)} + \frac{\gamma}{2}\|\lambda_D^i(T,\eta_D) - \lambda_N^i(\phi,\eta_N)\|^2_{\widehat{H}^{-\frac{1}{2}}(\Gamma_i)}, \tag{5a}$$

$$H_N(\eta_D,\eta_N) = \frac{1}{2}\|u_N(\phi,\eta_N) - T\|^2_{\widehat{H}^{\frac{1}{2}}(\Gamma_c)} + \frac{\gamma}{2}\|\lambda_D^i(T,\eta_D) - \lambda_N^i(\phi,\eta_N)\|^2_{\widehat{H}^{-\frac{1}{2}}(\Gamma_i)}, \tag{5b}$$

where $(u_D(T,\eta_D), \lambda_D^i(T,\eta_D), \lambda_D^c(T,\eta_D))$ and $(u_N(\phi,\eta_N), \lambda_N^i(\phi,\eta_N))$ are the unique solutions to (3) and (4), respectively. The game strategy involves two players with distinct objectives:

- **Player 1 (η_D)**: Minimizes the *Neumann gap* H_D, measuring misfit between computed $\lambda_D^c(T,\eta_D)$ and target ϕ on Γ_c.
- **Player 2 (η_N)**: Minimizes the *Dirichlet gap* H_N, measuring misfit between computed $u_N(\phi,\eta_N)$ and target T on Γ_c.

Both objectives include the coupling term $\frac{\gamma}{2}\|\lambda_D^i(T,\eta_D) - \lambda_N^i(\phi,\eta_N)\|^2$, which enables coordination by penalizing discrepancies in the Neumann data on Γ_i. Each player optimizes their control while considering the other's strategy fixed. A Nash equilibrium is reached when neither can unilaterally improve their outcome:

Definition 1. *A pair* (η_D, η_N) *is a* Nash equilibrium *if*

$$\begin{cases} H_D(\eta_D,\eta_N) \le H_D(\eta,\eta_N), & \forall \eta \in \widehat{H}^{\frac{1}{2}}(\Gamma_i), \\ H_N(\eta_D,\eta_N) \le H_N(\eta_D,\eta), & \forall \eta \in \widehat{H}^{\frac{1}{2}}(\Gamma_i). \end{cases} \tag{6}$$

At equilibrium, the coupling term is minimized, indicating the twin systems have reached consensus on the interface conditions.

1.3 Existence and Uniqueness of Nash Equilibrium

We now establish the fundamental well-posedness results for our Nash game formulation. The proof proceeds in two stages: first, we demonstrate the strong convexity and differentiability of the players' cost functionals [27]; second, we exploit these properties to prove existence and uniqueness of the Nash equilibrium through a combined optimization approach as in [6].

Proposition 1 (Well-Posedness of Player Objectives)**.** *The partial mappings $\eta_D \mapsto H_D(\eta_D, \eta_N)$ and $\eta_N \mapsto H_N(\eta_D, \eta_N)$ are twice Fréchet differentiable, quadratic, and γ-strongly convex functionals over $\widehat{H}^{\frac{1}{2}}(\Gamma_i)$.*

Proof. By the linearity of problems (P_D) and (P_N), we obtain the quadratic decompositions:

$$H_D(\eta_D, \eta_N) = \frac{1}{2} a_D^\gamma(\eta_D, \eta_D) - l_{D,\eta_N}^\gamma(\eta_D) + d_{D,\eta_N},$$
$$H_N(\eta_D, \eta_N) = \frac{1}{2} a_N^\gamma(\eta_N, \eta_N) - l_{N,\eta_D}^\gamma(\eta_N) + d_{N,\eta_D},$$

where a_D^γ and a_N^γ are symmetric bilinear forms on $\widehat{H}^{\frac{1}{2}}(\Gamma_i) \times \widehat{H}^{\frac{1}{2}}(\Gamma_i)$ defined by, for all $(\eta, h) \in (\widehat{H}^{\frac{1}{2}}(\Gamma_i))^2$:

$$a_D^\gamma(\eta, h) = a_D(\eta, h) + \gamma\big(\lambda_D^i(0,\eta), \lambda_D^i(0,h)\big)_{\widehat{H}^{-\frac{1}{2}}(\Gamma_i)},$$
$$a_N^\gamma(\eta, h) = a_N(\eta, h) + \gamma\big(\lambda_N^i(0,\eta), \lambda_N^i(0,h)\big)_{\widehat{H}^{-\frac{1}{2}}(\Gamma_i)},$$

where the component bilinear forms are:

$$a_D(\eta, h) = \big(\lambda_D^c(0,\eta), \lambda_D^c(0,h)\big)_{\widehat{H}^{-\frac{1}{2}}(\Gamma_c)},$$
$$a_N(\eta, h) = \big(u_N(0,\eta), u_N(0,h)\big)_{\widehat{H}^{\frac{1}{2}}(\Gamma_c)}.$$

The linear forms l_{D,η_N}^γ and l_{N,η_D}^γ on $\widehat{H}^{\frac{1}{2}}(\Gamma_i)$ are defined by, for all $h \in \widehat{H}^{\frac{1}{2}}(\Gamma_i)$:

$$l_{D,\eta_N}^\gamma(h) = -\big(\lambda_D^c(0,h), \lambda_D^c(T,0) - \phi\big)_{\widehat{H}^{-\frac{1}{2}}(\Gamma_c)} + \gamma\big(\lambda_D^i(0,h), \lambda_D^i(T,0) - \lambda_N^i(\phi,\eta_N)\big)_{\widehat{H}^{-\frac{1}{2}}(\Gamma_i)}, \quad (7a)$$
$$l_{N,\eta_D}^\gamma(h) = -\big(u_N(0,h), u_N(\phi,0) - T\big)_{\widehat{H}^{\frac{1}{2}}(\Gamma_c)} + \gamma\big(\lambda_N^i(0,h), \lambda_N^i(\phi,0) - \lambda_D^i(T,\eta_D)\big)_{\widehat{H}^{-\frac{1}{2}}(\Gamma_i)}. \quad (7b)$$

The affine terms are given by:

$$d_{D,\eta_N}^\gamma = \frac{1}{2}\|\lambda_D^c(T,0) - \phi\|^2_{H^{-\frac{1}{2}}(\Gamma_c)} + \frac{\gamma}{2}\|\lambda_D^i(T,0) - \lambda_N^i(\phi,\eta_N)\|^2_{H^{-\frac{1}{2}}(\Gamma_i)}, \quad (8a)$$
$$d_{N,\eta_D}^\gamma = \frac{1}{2}\|u_N(\phi,0) - T\|^2_{\widehat{H}^{\frac{1}{2}}(\Gamma_c)} + \frac{\gamma}{2}\|\lambda_D^i(T,\eta_D) - \lambda_N^i(\phi,0)\|^2_{H^{-\frac{1}{2}}(\Gamma_i)}. \quad (8b)$$

Since a_D^γ and a_N^γ are symmetric continuous bilinear forms, and l_{D,η_N}^γ and l_{N,η_D}^γ are continuous linear forms on $\widehat{H}^{\frac{1}{2}}(\Gamma_i)$, the partial mappings $\eta_D \mapsto H_D(\eta_D, \eta_N)$ and $\eta_N \mapsto H_N(\eta_D, \eta_N)$ are twice Fréchet differentiable with:

$$\langle H_D''(\eta_D, \eta_N) \cdot h, \tau\rangle = a_D^\gamma(h, \tau),$$
$$\langle H_N''(\eta_D, \eta_N) \cdot h, \tau\rangle = a_N^\gamma(h, \tau),$$

for all $(h, \tau) \in \widehat{H}^{\frac{1}{2}}(\Gamma_i) \times \widehat{H}^{\frac{1}{2}}(\Gamma_i)$. The γ-strongly convex follows from the positive definiteness of a_D and a_N over $\widehat{H}^{\frac{1}{2}}(\Gamma_i)$. □

Proposition 2 (Existence and Characterization of Nash Equilibrium)**.** *Assume the data completion problem* (1) *admits a solution* $\overline{v}$ *(i.e., the data are compatible). Then there exists a unique Nash equilibrium* $(\overline{\eta}_D, \overline{\eta}_N)$ *associated with* (5) *and* (6)*. Moreover, solving the data completion problem* (1) *is equivalent to finding this unique Nash equilibrium, which is given by* $(\overline{\eta}_C, \overline{\eta}_C)$ *with* $\overline{\eta}_C = \overline{v}|_{\Gamma_i}$*. In particular:*

$$u_D(T, \overline{\eta}_C) = u_N(\phi, \overline{\eta}_C) = \overline{v} \quad \text{in } \Omega,$$
$$\lambda_D^i(T, \overline{\eta}_C) = \lambda_N^i(\phi, \overline{\eta}_C) = \partial_n \overline{v}|_{\Gamma_i}.$$

Proof. Define the combined cost functional:

$$L^\gamma(\eta_D, \eta_N) = \frac{1}{2}\|\lambda_D^c(T, \eta_D) - \phi\|^2_{H^{-\frac{1}{2}}(\Gamma_c)} + \frac{1}{2}\|u_N(\phi, \eta_N) - T\|^2_{\widehat{H}^{\frac{1}{2}}(\Gamma_c)} + \frac{\gamma}{2}\|\lambda_D^i(T, \eta_D) - \lambda_N^i(\phi, \eta_N)\|^2_{H^{-\frac{1}{2}}(\Gamma_i)}.$$

Let $\overline{\eta}_C = \overline{v}|_{\Gamma_i}$. Then $L^\gamma(\overline{\eta}_C, \overline{\eta}_C) = 0$, implying that $(\overline{\eta}_C, \overline{\eta}_C)$ minimizes L^γ on $\widehat{H}^{\frac{1}{2}}(\Gamma_i) \times \widehat{H}^{\frac{1}{2}}(\Gamma_i)$. By uniqueness of the Cauchy solution:

$$\overline{v} = u_N(\phi, \overline{\eta}_C) = u_D(T, \overline{\eta}_C), \quad \partial_n \overline{v}|_{\Gamma_i} = \lambda_D^i(T, \overline{\eta}_C) = \lambda_N^i(\phi, \overline{\eta}_C).$$

Since L^γ is quadratic, twice differentiable, and strictly convex on $\widehat{H}^{\frac{1}{2}}(\Gamma_i) \times \widehat{H}^{\frac{1}{2}}(\Gamma_i)$, it has a unique minimum. The characterization of solution sets shows that any minimum of L^γ is a Nash equilibrium and vice versa. Therefore, the unique minimum of L^γ coincides with the unique Nash equilibrium $(\overline{\eta}_D, \overline{\eta}_N)$ defined by (5a), (5b), and (6). □

2 Stability and Error Bound Estimates with Noisy Measurements

The analysis developed in this section follows the robustness-oriented strategy introduced in [3]. Nevertheless, the present framework differs substantially from that setting. Here, the missing boundary trace is reconstructed through two coupled virtual controls within a Nash-game formulation. Consequently, the stability and error analysis must take into account not only the noise level δ and the Tikhonov regularization parameter α, but also the coupling parameter γ, which governs the interaction between the two players.

This section is devoted to the study of the stability properties of the regularized Nash game in the presence of noisy data. We derive explicit a priori error bounds for the noisy Nash equilibrium and clarify how the reconstruction error depends on δ, α, and γ.

2.1 Regularized Game for Noisy Data

Let us now consider the case of noisy data. Assume compatible data (T, ϕ) with corresponding Cauchy solution $\overline{v}$, and let $(T^\delta, \phi^\delta) \in \widehat{H}^{\frac{1}{2}}(\Gamma_c) \times H^{-\frac{1}{2}}(\Gamma_c)$ satisfy:

$$\|T - T^\delta\|^2_{\widehat{H}^{\frac{1}{2}}(\Gamma_c)} + \|\phi - \phi^\delta\|^2_{H^{-\frac{1}{2}}(\Gamma_c)} \leq \delta^2.$$

The noisy cost functionals are obtained by replacing (T, ϕ) with (T^δ, ϕ^δ) in the definitions from Section 1.2 and adding Tikhonov regularization:

$$H_D^{\gamma,\delta,\alpha}(\eta_D, \eta_N) = \frac{1}{2}a_D^{\alpha,\gamma}(\eta_D, \eta_D) - l_{D,\eta_N}^{\delta,\gamma}(\eta_D) + d_{D,\eta_N}^{\delta,\gamma}, \tag{9a}$$
$$H_N^{\gamma,\delta,\alpha}(\eta_D, \eta_N) = \frac{1}{2}a_N^{\alpha,\gamma}(\eta_N, \eta_N) - l_{N,\eta_D}^{\delta,\gamma}(\eta_N) + d_{N,\eta_D}^{\delta,\gamma}, \tag{9b}$$

where the regularized bilinear forms are:

$$a_D^{\alpha,\gamma}(\eta,h) = a_D^{\gamma}(\eta,h) + \alpha(\eta,h)_{\widehat{H}^{\frac{1}{2}}(\Gamma_i)},$$
$$a_N^{\alpha,\gamma}(\eta,h) = a_N^{\gamma}(\eta,h) + \alpha(\eta,h)_{\widehat{H}^{\frac{1}{2}}(\Gamma_i)},$$

and the linear forms and affine shifts are defined analogously to (7)-(8) with (T,ϕ) replaced by (T^δ,ϕ^δ).

Definition 2. *A pair $(\eta_D,\eta_N) \in (\widehat{H}^{\frac{1}{2}}(\Gamma_i))^2$ is a Nash equilibrium for the regularized problem with noisy data if*

$$\begin{cases} H_D^{\gamma,\delta,\alpha}(\eta_D,\eta_N) \le H_D^{\gamma,\delta,\alpha}(\eta,\eta_N), & \forall \eta \in \widehat{H}^{\frac{1}{2}}(\Gamma_i), \\ H_N^{\gamma,\delta,\alpha}(\eta_D,\eta_N) \le H_N^{\gamma,\delta,\alpha}(\eta_D,\eta), & \forall \eta \in \widehat{H}^{\frac{1}{2}}(\Gamma_i). \end{cases} \tag{10}$$

We finish with existence and uniqueness results for the noisy Nash equilibrium.

Proposition 3 (Well-Posedness of Regularized Nash Game)**.** *For any $(\delta,\alpha,\gamma) \in \mathbb{R}_+ \times (\mathbb{R}_+^*)^2$, there exists a unique noisy regularized Nash equilibrium $(\overline{\eta}_D^{\delta,\alpha},\overline{\eta}_N^{\delta,\alpha})$ defined by (9) and (10).*

Proof. The proof follows the same variational arguments as Proposition 2, with the Tikhonov regularization ensuring uniform coercivity of the bilinear forms. □

2.2 Stability Estimates

We analyze the behavior of the Nash equilibrium as the noise level δ decrease and provide explicit estimates of the error bounds . The analysis proceeds by first establishing error estimates for the regularization method, then analyzing stability with respect to data noise, and finally combining these results to obtain error bound rates. Throughout this section, $a \lesssim b$ signifies $a \le Cb$ for some constant $C > 0$ independent of γ, δ, and α.

Lemma 1 (Density and Approximation Estimates)**.** *Assume that the data completion problem (1) admits a unique solution $\overline{v} \in H^1(\Omega)$ for a given compatible pair of data $(T,\phi) \in \widehat{H}^{\frac{1}{2}}(\Gamma_c) \times \widehat{H}^{-\frac{1}{2}}(\Gamma_c)$. Define $\overline{\eta}_C = \overline{v}|_{\Gamma_i}$ and let ε and M be two positive real numbers such that $\varepsilon < M$. Then there exist $(\omega_N,\omega_D) \in \widehat{H}^{\frac{1}{2}}(\Gamma_c) \times \widehat{H}^{-\frac{1}{2}}(\Gamma_c)$, depending only on ε, M and the exact missing data $\overline{\eta}_C$ such that the following inequalities hold for all $\alpha \in [\varepsilon, M]$:*

$$(\overline{\eta}_C, \overline{\eta}_N^\alpha - \overline{\eta}_C)_{\widehat{\mathbb{H}}^{\frac{1}{2}}(\Gamma_i)} \le \|\omega_N\|_{\widehat{H}^{\frac{1}{2}}(\Gamma_c)} \|u_N(0, \overline{\eta}_N^\alpha - \overline{\eta}_C)\|_{\widehat{\mathbb{H}}^{\frac{1}{2}}(\Gamma_c)} \tag{11a}$$
$$(\overline{\eta}_C, \overline{\eta}_D^\alpha - \overline{\eta}_C)_{\widehat{\mathbb{H}}^{\frac{1}{2}}(\Gamma_i)} \le \|\omega_D\|_{\widehat{H}^{-\frac{1}{2}}(\Gamma_c)} \|\lambda_D^c(0, \overline{\eta}_D^\alpha - \overline{\eta}_C)\|_{\widehat{\mathbb{H}}^{-\frac{1}{2}}(\Gamma_c)}, \tag{11b}$$

Proof. Let $\varphi \in \widehat{\mathbb{H}}^{\frac{1}{2}}(\Gamma_c)$, $W(\varphi, S_{DN}^i \overline{\eta})$ the unique weak solution of:

$$\begin{cases} -\Delta W = 0, & \text{in } \Omega, \\ W = \varphi, & \text{on } \Gamma_c, \\ \partial_n W = S_{DN}^i \overline{\eta}_C, & \text{on } \Gamma_i, \\ W = 0, & \text{on } \Gamma_0, \end{cases} \tag{12}$$

and define

$$S_{S_{DN}^i \overline{\eta}_C} = \left\{ \mu \in \widehat{H}^{\frac{1}{2}}(\Gamma_i) \text{ such that } \exists \varphi \in \widehat{H}^{\frac{1}{2}}(\Gamma_c) \text{ with } \mu = W(\varphi, S_{DN}^i \overline{\eta}_C)|_{\Gamma_i} \right\},$$

where W is the unique weak solution of (12).

Case 1: $0 \in S_{S^i_{DN}\overline{\eta}_C}$. There exists $\varphi \in \widehat{H}^{\frac{1}{2}}(\Gamma_c)$ such that $W(\varphi, S^i_{DN}\overline{\eta}_C)_{|\Gamma_i} = 0$. Using the weak formulations of (12), (3) and (4), we have:

$$\begin{aligned}
(\overline{\eta}_C, \overline{\eta}^\alpha_N - \overline{\eta}_C)_{\widehat{\mathbb{H}}^{\frac{1}{2}}(\Gamma_i)} &= -\langle \partial_n W(\varphi, S^i_{DN}\overline{\eta}_C), u_N(0, \overline{\eta}^\alpha_N - \overline{\eta}_C)\rangle_{\Gamma_c} \\
&= -(\omega_N, u_N(0, \overline{\eta}^\alpha_N - \overline{\eta}_C))_{\widehat{H}^{\frac{1}{2}}(\Gamma_c)}, \\
(\overline{\eta}_C, \overline{\eta}^\alpha_D - \overline{\eta}_C)_{\widehat{\mathbb{H}}^{\frac{1}{2}}(\Gamma_i)} &= \langle \lambda^c_D(0, \overline{\eta}^\alpha_D - \overline{\eta}_C), W(\varphi, S^i_{DN}\overline{\eta}_C)\rangle_{\Gamma_c} \\
&= (\omega_D, \lambda^c_D(0, \overline{\eta}^\alpha_D - \overline{\eta}_C))_{\widehat{H}^{-\frac{1}{2}}(\Gamma_c)},
\end{aligned}$$

where $\omega_N = S^c_{ND}(\partial_n W(\varphi, S^i_{DN}\overline{\eta}_C))$ and $\omega_D = S^c_{DN}(W(\varphi, S^i_{DN}\overline{\eta}_C))$. Then by Cauchy-Schwarz:

$$\begin{aligned}
(\overline{\eta}_C, \overline{\eta}^\alpha_N - \overline{\eta}_C)_{\widehat{\mathbb{H}}^{\frac{1}{2}}(\Gamma_i)} &\leq \|\omega_N\|_{\widehat{H}^{\frac{1}{2}}(\Gamma_c)} \|u_N(0, \overline{\eta}^\alpha_N - \overline{\eta}_C)\|_{\widehat{\mathbb{H}}^{\frac{1}{2}}(\Gamma_c)}, \\
(\overline{\eta}_C, \overline{\eta}^\alpha_D - \overline{\eta}_C)_{\widehat{\mathbb{H}}^{\frac{1}{2}}(\Gamma_i)} &\leq \|\omega_D\|_{\widehat{H}^{-\frac{1}{2}}(\Gamma_c)} \|\lambda^c_D(0, \overline{\eta}^\alpha_D - \overline{\eta}_C)\|_{\widehat{\mathbb{H}}^{-\frac{1}{2}}(\Gamma_c)}.
\end{aligned}$$

Case 2: $0 \notin S_{S^i_{DN}\overline{\eta}_C}$. Since $S_{S^i_{DN}\overline{\eta}_C}$ is dense in $\widehat{H}^{\frac{1}{2}}(\Gamma_i)$ (see [3, 24]), there exists a sequence $(\mu_n)_{n\in\mathbb{N}} \subset S_{S^i_{DN}\overline{\eta}_C}$ converging strongly to zero in $\widehat{H}^{\frac{1}{2}}(\Gamma_i)$. For each $\mu_n \in S_{S^i_{DN}\overline{\eta}_C}$, there exists $\varphi_n \in \widehat{H}^{\frac{1}{2}}(\Gamma_c)$ such that $\mu_n = W(\varphi_n, S^i_{DN}\overline{\eta}_C)$ for all $n \in \mathbb{N}$. Using the weak formulations:

$$\begin{aligned}
(\overline{\eta}_C, \overline{\eta}^\alpha_N - \overline{\eta}_C)_{\widehat{\mathbb{H}}^{\frac{1}{2}}(\Gamma_i)} &= -\langle \partial_n W(\varphi_n, S^i_{DN}\overline{\eta}_C), u_N(0, \overline{\eta}^\alpha_N - \overline{\eta}_C)\rangle_{\Gamma_c} + \langle \lambda^i_N(0, \overline{\eta}^\alpha_N - \overline{\eta}_C), \mu_n\rangle_{\Gamma_i} \\
&= -(\omega^n_N, u_N(0, \overline{\eta}^\alpha_N - \overline{\eta}_C))_{\widehat{\mathbb{H}}^{\frac{1}{2}}(\Gamma_c)} + \langle \lambda^i_N(0, \overline{\eta}^\alpha_N - \overline{\eta}_C), \mu_n\rangle_{\Gamma_i}, \\
(\overline{\eta}_C, \overline{\eta}^\alpha_D - \overline{\eta}_C)_{\widehat{\mathbb{H}}^{\frac{1}{2}}(\Gamma_i)} &= \langle \lambda^c_D(0, \overline{\eta}^\alpha_D - \overline{\eta}_C), \varphi_n\rangle_{\Gamma_c} + \langle \lambda^i_D(0, \overline{\eta}^\alpha_D - \overline{\eta}_C), \mu_n\rangle_{\Gamma_i} \\
&= (\omega^n_D, \lambda^c_D(0, \overline{\eta}^\alpha_D - \overline{\eta}_C))_{\widehat{\mathbb{H}}^{-\frac{1}{2}}(\Gamma_c)} + \langle \lambda^i_D(0, \overline{\eta}^\alpha_D - \overline{\eta}_C), \mu_n\rangle_{\Gamma_i},
\end{aligned}$$

where $\omega^n_N = S^c_{ND}(\partial_n W(\varphi_n, S^i_{DN}\overline{\eta}_C))$ and $\omega^n_D = S^c_{DN}(\varphi_n)$. For all $n \in \mathbb{N}$:

$$\begin{aligned}
(\overline{\eta}_C, \overline{\eta}^\alpha_N - \overline{\eta}_C)_{\widehat{\mathbb{H}}^{\frac{1}{2}}(\Gamma_i)} &\leq \|\omega^n_N\|_{\widehat{H}^{\frac{1}{2}}(\Gamma_c)} \|u_N(0, \overline{\eta}^\alpha_N - \overline{\eta}_C)\|_{\widehat{\mathbb{H}}^{\frac{1}{2}}(\Gamma_c)} \\
&\quad + \|\lambda^i_N(0, \overline{\eta}^\alpha_N - \overline{\eta}_C)\|_{\widehat{H}^{-\frac{1}{2}}(\Gamma_i)} \|\mu_n\|_{\widehat{H}^{\frac{1}{2}}(\Gamma_i)}, \qquad (13) \\
(\overline{\eta}_C, \overline{\eta}^\alpha_D - \overline{\eta}_C)_{\widehat{\mathbb{H}}^{\frac{1}{2}}(\Gamma_i)} &\leq \|\omega^n_D\|_{\widehat{H}^{-\frac{1}{2}}(\Gamma_c)} \|\lambda^c_D(0, \overline{\eta}^\alpha_D - \overline{\eta}_C)\|_{\widehat{\mathbb{H}}^{-\frac{1}{2}}(\Gamma_c)} \\
&\quad + \|\lambda^i_D(0, \overline{\eta}^\alpha_D - \overline{\eta}_C)\|_{\widehat{H}^{-\frac{1}{2}}(\Gamma_i)} \|\mu_n\|_{\widehat{H}^{\frac{1}{2}}(\Gamma_i)}. \qquad (14)
\end{aligned}$$

Since (μ_n) converges strongly to zero in $\widehat{H}^{-\frac{1}{2}}(\Gamma_i)$, it follows that for any $\alpha > 0$ there exist integers $(KD_\alpha, KN_\alpha) \in \mathbb{N}^2$ such that:

$$\|\lambda^i_N(0, \overline{\eta}^\alpha_N - \overline{\eta}_C)\|_{\widehat{H}^{-\frac{1}{2}}(\Gamma_i)} \|\mu_{KN_\alpha}\|_{\widehat{H}^{\frac{1}{2}}(\Gamma_i)} \leq \|\omega^{KN_\alpha}_N\|_{\widehat{H}^{\frac{1}{2}}(\Gamma_c)} \|u_N(0, \overline{\eta}^\alpha_N - \overline{\eta}_C)\|_{\widehat{\mathbb{H}}^{\frac{1}{2}}(\Gamma_c)}, \qquad (15)$$

$$\|\lambda^i_D(0, \overline{\eta}^\alpha_D - \overline{\eta}_C)\|_{\widehat{H}^{-\frac{1}{2}}(\Gamma_i)} \|\mu_{KD_\alpha}\|_{\widehat{H}^{\frac{1}{2}}(\Gamma_i)} \leq \|\omega^{KD_\alpha}_D\|_{\widehat{H}^{-\frac{1}{2}}(\Gamma_c)} \|\lambda^c_D(0, \overline{\eta}^\alpha_D - \overline{\eta}_C)\|_{\widehat{\mathbb{H}}^{-\frac{1}{2}}(\Gamma_c)}. \qquad (16)$$

We denote by KD_α (respectively KN_α) the smallest integer for which inequality (15) (respectively (16)) is satisfied. Combining inequalities (13) and (14) with (15) and (16), we infer that:

$$\begin{aligned}
(\overline{\eta}_C, \overline{\eta}^\alpha_N - \overline{\eta}_C)_{\widehat{\mathbb{H}}^{\frac{1}{2}}(\Gamma_i)} &\leq 2\|\omega^{KN_\alpha}_N\|_{\widehat{H}^{\frac{1}{2}}(\Gamma_c)} \|u_N(0, \overline{\eta}^\alpha_N - \overline{\eta}_C)\|_{\widehat{\mathbb{H}}^{\frac{1}{2}}(\Gamma_c)}, \\
(\overline{\eta}_C, \overline{\eta}^\alpha_D - \overline{\eta}_C)_{\widehat{\mathbb{H}}^{\frac{1}{2}}(\Gamma_i)} &\leq 2\|\omega^{KD_\alpha}_D\|_{\widehat{H}^{-\frac{1}{2}}(\Gamma_c)} \|\lambda^c_D(0, \overline{\eta}^\alpha_D - \overline{\eta}_C)\|_{\widehat{\mathbb{H}}^{-\frac{1}{2}}(\Gamma_c)}.
\end{aligned}$$

Using the same argument as in the proof of Lemma 4.4 in [3], the families $(KN_\alpha)_{\alpha\in[\varepsilon,M]}$ and $(KD_\alpha)_{\alpha\in[\varepsilon,M]}$ are uniformly bounded. Consequently, we may define

$$\overline{KN}_{\varepsilon,M} = \max_{\alpha\in[\varepsilon,M]} KN_\alpha, \quad \overline{KD}_{\varepsilon,M} = \max_{\alpha\in[\varepsilon,M]} KD_\alpha,$$

and select $\omega_{\overline{KN}_{\varepsilon,M}}$ and $\omega_{\overline{KD}_{\varepsilon,M}}$ such that

$$\|\omega_{\overline{KN}_{\varepsilon,M}}\|_{\widehat{H}^{\frac{1}{2}}(\Gamma_c)} = \max_{0\le n\le \overline{KN}_{\varepsilon,M}} \|\omega_N^n\|_{\widehat{H}^{\frac{1}{2}}(\Gamma_c)},$$
$$\|\omega_{\overline{KD}_{\varepsilon,M}}\|_{\widehat{H}^{-\frac{1}{2}}(\Gamma_c)} = \max_{0\le n\le \overline{KD}_{\varepsilon,M}} \|\omega_D^n\|_{\widehat{H}^{-\frac{1}{2}}(\Gamma_c)}.$$

This completes the proof. □

Lemma 2. *Let ε, and M be two positive real numbers such that $\varepsilon < M$. Under the assumptions of Lemma 1, if $\overline{v}$ is the unique solution of the data completion problem (1), then there exist $(\omega_N, \omega_D) \in \widehat{H}^{\frac{1}{2}}(\Gamma_c) \times \widehat{H}^{-\frac{1}{2}}(\Gamma_c)$, depending only on ε, M and the exact missing data $\overline{\eta}_C$ such that the following inequality holds for all $\alpha \in [\varepsilon, M]$:*

$$\|u_N(0, \overline{\eta}_N^\alpha - \overline{\eta}_C)\|_{\widehat{H}^{\frac{1}{2}}(\Gamma_c)} + \|\lambda_D^c(0, \overline{\eta}_D^\alpha - \overline{\eta}_C)\|_{\widehat{\mathbb{H}}^{-\frac{1}{2}}(\Gamma_c)} \lesssim \alpha \left(\|\omega_D\|_{\widehat{H}^{-\frac{1}{2}}(\Gamma_c)} + \|\omega_N\|_{\widehat{H}^{\frac{1}{2}}(\Gamma_c)} \right). \quad (17)$$

Proof. Assume the hypotheses of Lemma 1 hold. Let $\overline{v}$ be the unique solution of (1) and define $\overline{\eta}_C = \overline{v}_{|\Gamma_i}$. We begin with the optimality conditions from the Nash equilibrium formulation (6):

$$a_D^{\alpha,\gamma}(\overline{\eta}_D^\alpha, h) = l^\gamma_{D,\overline{\eta}_N^\alpha}(h), \quad \forall h \in \widehat{H}^{\frac{1}{2}}(\Gamma_i),$$
$$a_D^{\gamma}(\overline{\eta}_C, h) = l^\gamma_{D,\overline{\eta}_C}(h), \quad \forall h \in \widehat{H}^{\frac{1}{2}}(\Gamma_i),$$
$$a_N^{\alpha,\gamma}(\overline{\eta}_N^\alpha, h) = l^\gamma_{N,\overline{\eta}_D^\alpha}(h), \quad \forall h \in \widehat{H}^{\frac{1}{2}}(\Gamma_i),$$
$$a_N^{\gamma}(\overline{\eta}_C, h) = l^\gamma_{N,\overline{\eta}_C}(h), \quad \forall h \in \widehat{H}^{\frac{1}{2}}(\Gamma_i).$$

Define the approximation errors:

$$e_{DC}^\alpha = \overline{\eta}_D^\alpha - \overline{\eta}_C,$$
$$e_{NC}^\alpha = \overline{\eta}_N^\alpha - \overline{\eta}_C.$$

Subtracting the corresponding equations yields the error relations:

$$a_D^\gamma(e_{DC}^\alpha, e_{DC}^\alpha) + \alpha(\overline{\eta}_D^\alpha, e_{DC}^\alpha)_{H^{\frac{1}{2}}(\Gamma_i)} = l^\gamma_{D,\overline{\eta}_N^\alpha}(e_{DC}^\alpha) - l^\gamma_{D,\overline{\eta}_C}(e_{DC}^\alpha), \quad (18a)$$
$$a_N^\gamma(e_{NC}^\alpha, e_{NC}^\alpha) + \alpha(\overline{\eta}_N^\alpha, e_{NC}^\alpha)_{H^{\frac{1}{2}}(\Gamma_i)} = l^\gamma_{N,\overline{\eta}_D^\alpha}(e_{NC}^\alpha) - l^\gamma_{N,\overline{\eta}_C}(e_{NC}^\alpha). \quad (18b)$$

The right-hand sides satisfy the bounds:

$$\begin{aligned} l^\gamma_{D,\overline{\eta}_N^\alpha}(e_{DC}^\alpha) - l^\gamma_{D,\overline{\eta}_C}(e_{DC}^\alpha) &= \gamma(\lambda_N^i(0, e_{NC}^\alpha), \lambda_D^i(0, e_{DC}^\alpha))_{\widehat{H}^{\frac{1}{2}}(\Gamma_i)} \\ &\le \frac{\gamma}{2}\|\lambda_N^i(0, e_{NC}^\alpha)\|^2_{H^{-\frac{1}{2}}(\Gamma_i)} + \frac{\gamma}{2}\|\lambda_D^i(0, e_{DC}^\alpha)\|^2_{H^{-\frac{1}{2}}(\Gamma_i)}, \quad (19a) \\ l^\gamma_{N,\overline{\eta}_D^\alpha}(e_{NC}^\alpha) - l^\gamma_{N,\overline{\eta}_C}(e_{NC}^\alpha) &= \gamma(\lambda_D^i(0, e_{DC}^\alpha), \lambda_N^i(0, e_{NC}^\alpha))_{\widehat{H}^{\frac{1}{2}}(\Gamma_i)} \\ &\le \frac{\gamma}{2}\|\lambda_N^i(0, e_{NC}^\alpha)\|^2_{H^{-\frac{1}{2}}(\Gamma_i)} + \frac{\gamma}{2}\|\lambda_D^i(0, e_{DC}^\alpha)\|^2_{H^{-\frac{1}{2}}(\Gamma_i)}. \quad (19b) \end{aligned}$$

Combining (18)-(19), we obtain:

$$\begin{aligned} a_D(e^\alpha_{DC}, e^\alpha_{DC}) + a_N(e^\alpha_{NC}, e^\alpha_{NC}) &\leq -\alpha(\overline{\eta}^\alpha_D, e^\alpha_{DC})_{\widehat{H}^{\frac{1}{2}}(\Gamma_i)} - \alpha(\overline{\eta}^\alpha_N, e^\alpha_{NC})_{\widehat{H}^{\frac{1}{2}}(\Gamma_i)} \\ &= -\alpha\|e^\alpha_{DC}\|^2_{\widehat{H}^{\frac{1}{2}}(\Gamma_i)} - \alpha\|e^\alpha_{NC}\|^2_{\widehat{H}^{\frac{1}{2}}(\Gamma_i)} \\ &\quad - \alpha(\overline{\eta}_C, e^\alpha_{DC})_{\widehat{H}^{\frac{1}{2}}(\Gamma_i)} - \alpha(\overline{\eta}_C, e^\alpha_{NC})_{\widehat{H}^{\frac{1}{2}}(\Gamma_i)}. \end{aligned} \tag{20}$$

Now applying the density estimates from Lemma 1 (see inequalities (11a)-(11b)):

$$\begin{aligned} &\|\lambda^c_D(0, e^\alpha_{DC})\|^2_{\widehat{H}^{-\frac{1}{2}}(\Gamma_c)} + \|u_N(0, e^\alpha_{NC})\|^2_{\widehat{H}^{\frac{1}{2}}(\Gamma_c)} \\ &\qquad \leq \alpha\|\omega_D\|_{\widehat{H}^{-\frac{1}{2}}(\Gamma_c)}\|\lambda^c_D(0, e^\alpha_{DC})\|_{\widehat{H}^{-\frac{1}{2}}(\Gamma_c)} \\ &\qquad\quad + \alpha\|\omega_N\|_{\widehat{H}^{\frac{1}{2}}(\Gamma_c)}\|u_N(0, e^\alpha_{NC})\|_{\widehat{H}^{\frac{1}{2}}(\Gamma_c)}. \end{aligned}$$

This inequality implies the desired bound (17), completing the proof. □

Proposition 4 (Error Bounds for Regularized Controls)**.** *Let ε, and M be two positive real numbers such that $\varepsilon < M$. Under the assumptions of Lemma 1, if $\overline{v}$ is the unique solution of the data completion problem (1), then there exist $(\omega_N, \omega_D) \in \widehat{H}^{\frac{1}{2}}(\Gamma_c) \times \widehat{H}^{-\frac{1}{2}}(\Gamma_c)$, depending only on ε, M and the exact missing data $\overline{\eta}_C$ such that the following inequality holds for all $\alpha \in [\varepsilon, M]$:*

$$\|\overline{\eta}^\alpha_D - \overline{\eta}_C\|_{\widehat{\mathbb{H}}^{\frac{1}{2}}(\Gamma_c)} + \|\overline{\eta}^\alpha_N - \overline{\eta}_C\|_{\widehat{H}^{\frac{1}{2}}(\Gamma_c)} \lesssim \sqrt{\alpha}\left(\|\omega_D\|_{\widehat{H}^{-\frac{1}{2}}(\Gamma_c)} + \|\omega_N\|_{\widehat{H}^{\frac{1}{2}}(\Gamma_c)}\right).$$

Proof. The result follows immediately by combining the bound from Lemma 2 with the energy estimate (20). □

Next, we analyze the stability of the Nash equilibrium with respect to data perturbations.

Proposition 5 (Stability Estimates)**.** *Assume there exists a unique solution $\overline{v} \in H^1(\Omega)$ to the data completion problem (1) for compatible data $(T, \phi) \in \widehat{H}^{\frac{1}{2}}(\Gamma_c) \times H^{-\frac{1}{2}}(\Gamma_c)$. Let (T^δ, ϕ^δ) satisfy:*

$$\|T - T^\delta\|^2_{\widehat{H}^{\frac{1}{2}}(\Gamma_c)} + \|\phi - \phi^\delta\|^2_{H^{-\frac{1}{2}}(\Gamma_c)} \leq \delta^2.$$

Let $\ell(\delta, \gamma, \alpha) := \sqrt{\dfrac{\delta^2}{\alpha} + \dfrac{\gamma^2\delta^2}{\alpha^2}}$. Then for any $(\delta, \alpha, \gamma) \in \mathbb{R}_+ \times (\mathbb{R}^*_+)^2$, the following estimates hold:

$$\|\overline{\eta}^{\delta,\alpha}_D - \overline{\eta}^\alpha_D\|_{\widehat{H}^{\frac{1}{2}}(\Gamma_i)} + \|\overline{\eta}^{\delta,\alpha}_N - \overline{\eta}^\alpha_N\|_{\widehat{H}^{\frac{1}{2}}(\Gamma_i)} \lesssim \ell(\delta, \gamma, \alpha), \tag{21a}$$

$$\|u_D(T^\delta, \overline{\eta}^{\delta,\alpha}_D) - u_D(T, \overline{\eta}^\alpha_D)\|_{H^1(\Omega)} \lesssim \ell(\delta, \gamma, \alpha) + \delta, \tag{21b}$$

$$\|u_N(\phi^\delta, \overline{\eta}^{\delta,\alpha}_N) - u_N(\phi, \overline{\eta}^\alpha_N)\|_{H^1(\Omega)} \lesssim \ell(\delta, \gamma, \alpha) + \delta. \tag{21c}$$

Moreover, as $\delta \to 0$, the noisy Nash equilibrium converges strongly to the regularized equilibrium.

Proof. Define the error terms:

$$e^{\delta,\alpha}_D = \overline{\eta}^{\delta,\alpha}_D - \overline{\eta}^\alpha_D, \quad e^{\delta,\alpha}_N = \overline{\eta}^{\delta,\alpha}_N - \overline{\eta}^\alpha_N.$$

From the optimality conditions, we obtain the error equations:

$$\begin{aligned} a^{\alpha,\gamma}_D(e^{\delta,\alpha}_D, e^{\delta,\alpha}_D) &= l^{\delta,\gamma}_{D,\overline{\eta}^{\delta,\alpha}_N}(e^{\delta,\alpha}_D) - l^\gamma_{D,\overline{\eta}^\alpha_N}(e^{\delta,\alpha}_D), \\ a^{\alpha,\gamma}_N(e^{\delta,\alpha}_N, e^{\delta,\alpha}_N) &= l^{\delta,\gamma}_{N,\overline{\eta}^{\delta,\alpha}_D}(e^{\delta,\alpha}_N) - l^\gamma_{N,\overline{\eta}^\alpha_D}(e^{\delta,\alpha}_N). \end{aligned}$$

Using the coercivity:

$$a_D^{\alpha,\gamma}(e_D^{\delta,\alpha}, e_D^{\delta,\alpha}) = \|\lambda_D^c(0, e_D^{\delta,\alpha})\|^2_{H^{-\frac{1}{2}}(\Gamma_c)} + \alpha\|e_D^{\delta,\alpha}\|^2_{\widehat{H}^{\frac{1}{2}}(\Gamma_i)} + \gamma\|\lambda_D^i(0, e_D^{\delta,\alpha})\|^2_{H^{-\frac{1}{2}}(\Gamma_i)},$$

and estimating the right-hand side:

$$\begin{aligned}
&a_D^{\alpha,\gamma}(e_D^{\delta,\alpha}, e_D^{\delta,\alpha}) \\
&\quad= \big(\lambda_D^c(0, e_D^{\delta,\alpha}), \lambda_D^c(T - T^\delta, 0) + \phi^\delta - \phi\big)_{\widehat{H}^{-\frac{1}{2}}(\Gamma_c)} \\
&\qquad+ \gamma\big(\lambda_D^i(0, e_D^{\delta,\alpha}), \lambda_D^i(T - T^\delta, 0) - \lambda_N^i(\phi, \overline{\eta}_N^\alpha) + \lambda_N^i(\phi^\delta, \overline{\eta}_N^{\delta,\alpha})\big)_{\widehat{H}^{-\frac{1}{2}}(\Gamma_i)} \\
&\quad\underset{\text{CS}}{\leq} \|\lambda_D^c(0, e_D^{\delta,\alpha})\|_{\widehat{H}^{-\frac{1}{2}}(\Gamma_c)}\big(\|\lambda_D^c(T - T^\delta, 0)\|_{\widehat{H}^{-\frac{1}{2}}(\Gamma_c)} + \|\phi^\delta - \phi\|_{\widehat{H}^{-\frac{1}{2}}(\Gamma_c)}\big) \\
&\qquad+ \gamma\|\lambda_D^i(0, e_D^{\delta,\alpha})\|_{\widehat{H}^{-\frac{1}{2}}(\Gamma_i)} \\
&\qquad\quad\times \big(\|\lambda_D^i(T - T^\delta, 0)\|_{\widehat{H}^{-\frac{1}{2}}(\Gamma_i)} + \|\lambda_N^i(\phi^\delta - \phi, 0)\|_{\widehat{H}^{-\frac{1}{2}}(\Gamma_i)} + \|\lambda_N^i(0, e_N^{\delta,\alpha})\|_{\widehat{H}^{-\frac{1}{2}}(\Gamma_i)}\big).
\end{aligned}$$

Thus

$$\begin{aligned}
&a_D^{\alpha,\gamma}(e_D^{\delta,\alpha}, e_D^{\delta,\alpha}) - \gamma\|\lambda_D^i(0, e_D^{\delta,\alpha})\|_{H^{-\frac{1}{2}}(\Gamma_i)}\|\lambda_N^i(0, e_N^{\delta,\alpha})\|_{\widehat{H}^{-\frac{1}{2}}(\Gamma_i)} \\
&\qquad\underset{\text{Cont.}}{\lesssim} \delta\,\left(\|\lambda_D^c(0, e_D^{\delta,\alpha})\|_{\widehat{H}^{-\frac{1}{2}}(\Gamma_c)} + \gamma\,\|e_D^{\delta,\alpha}\|_{\widehat{H}^{\frac{1}{2}}(\Gamma_i)}\right)
\end{aligned}$$

Using the definition of $a_D^{\alpha,\gamma}$ and the Young's inequality, we have:

$$\frac{\alpha}{2}\|e_D^{\delta,\alpha}\|^2_{\widehat{H}^{\frac{1}{2}}(\Gamma_i)} + \frac{\gamma}{2}\|\lambda_D^i(0, e_D^{\delta,\alpha})\|^2_{H^{-\frac{1}{2}}(\Gamma_i)} - \frac{\gamma}{2}\|\lambda_N^i(0, e_N^{\delta,\alpha})\|^2_{H^{-\frac{1}{2}}(\Gamma_i)} \lesssim \frac{\delta^2}{\alpha} + \frac{\gamma^2\delta^2}{\alpha^2}. \tag{22}$$

For the Neumann player, we have

$$a_N^{\alpha,\gamma}(e_N^{\delta,\alpha}, e_N^{\delta,\alpha}) = \|S_{DN}^c(u_N(0, e_N^{\delta,\alpha}))\|^2_{H^{-\frac{1}{2}}(\Gamma_c)} + \alpha\|e_N^{\delta,\alpha}\|^2_{\widehat{H}^{\frac{1}{2}}(\Gamma_i)} + \gamma\|\lambda_N^i(0, e_N^{\delta,\alpha})\|^2_{\widehat{H}^{-\frac{1}{2}}(\Gamma_i)},$$

and estimating yields:

$$\frac{\alpha}{2}\|e_N^{\delta,\alpha}\|^2_{\widehat{H}^{\frac{1}{2}}(\Gamma_i)} + \frac{\gamma}{2}\|\lambda_N^i(0, e_N^{\delta,\alpha})\|^2_{\widehat{H}^{-\frac{1}{2}}(\Gamma_i)} - \frac{\gamma}{2}\|\lambda_D^i(0, e_D^{\delta,\alpha})\|^2_{\widehat{H}^{-\frac{1}{2}}(\Gamma_i)} \lesssim \frac{\delta^2}{\alpha} + \frac{\gamma^2\delta^2}{\alpha^2}. \tag{23}$$

Now, adding inequalities (22) and (23) and absorbing the coupling terms gives:

$$\|e_D^{\delta,\alpha}\|_{\widehat{H}^{\frac{1}{2}}(\Gamma_i)} + \|e_N^{\delta,\alpha}\|_{\widehat{H}^{\frac{1}{2}}(\Gamma_i)} \lesssim \sqrt{\frac{\delta^2}{\alpha} + \frac{\gamma^2\delta^2}{\alpha^2}} = \ell(\delta, \gamma, \alpha),$$

which proves (21a). For the Dirichlet solution, by triangle inequality and continuity:

$$\begin{aligned}
&\|u_D(T^\delta, \overline{\eta}_D^{\delta,\alpha}) - u_D(T, \overline{\eta}_D^\alpha)\|_{H^1(\Omega)} \\
&\quad\underset{\text{Triangle}}{\leq} \|u_D(T^\delta, \overline{\eta}_D^{\delta,\alpha}) - u_D(T, \overline{\eta}_D^{\delta,\alpha})\|_{H^1(\Omega)} + \|u_D(T, \overline{\eta}_D^{\delta,\alpha}) - u_D(T, \overline{\eta}_D^\alpha)\|_{H^1(\Omega)} \\
&\quad= \|u_D(T^\delta - T, 0)\|_{H^1(\Omega)} + \|u_D(0, e_D^{\delta,\alpha})\|_{H^1(\Omega)} \\
&\quad\underset{\text{Continuity}}{\lesssim} \|T - T^\delta\|_{\widehat{H}^{\frac{1}{2}}(\Gamma_c)} + \|e_D^{\delta,\alpha}\|_{\widehat{H}^{\frac{1}{2}}(\Gamma_i)} \\
&\quad\lesssim \delta + \ell(\delta, \gamma, \alpha),
\end{aligned}$$

proving (21b). The estimate (21c) follows similarly. □

2.2.1 Convergence Analysis and Error Bound Estimates

We combine the previous results to obtain the main convergence proposition.

Proposition 6 (Robust Convergence of Noisy Nash Equilibrium)**.** *Assume there exists a unique solution $\overline{v} \in H^1(\Omega)$ to the Cauchy problem for compatible data $(T, \phi) \in \widehat{H}^{\frac{1}{2}}(\Gamma_c) \times H^{-\frac{1}{2}}(\Gamma_c)$. Let $(\delta, \alpha, \gamma) \in \mathbb{R}_+ \times (\mathbb{R}_+^*)^2$ and let $(T^\delta, \phi^\delta) \in \widehat{H}^{\frac{1}{2}}(\Gamma_c) \times H^{-\frac{1}{2}}(\Gamma_c)$ be noisy data satisfying:*

$$\|T - T^\delta\|^2_{\widehat{H}^{\frac{1}{2}}(\Gamma_c)} + \|\phi - \phi^\delta\|^2_{H^{-\frac{1}{2}}(\Gamma_c)} \leq \delta^2.$$

Then there exists a unique noisy Nash equilibrium $(\overline{\eta}_D^{\delta,\alpha}, \overline{\eta}_N^{\delta,\alpha})$ defined by (9) and (10) with the following properties:

(i) The noisy equilibrium converges strongly to the exact equilibrium $(\overline{\eta}_C, \overline{\eta}_C)$ as $\alpha \to 0$ and $\dfrac{\delta}{\sqrt{\alpha}} \to 0$.

(ii) The solutions $u_D(T^\delta, \overline{\eta}_D^{\delta,\alpha})$ and $u_N(\phi^\delta, \overline{\eta}_N^{\delta,\alpha})$ of (3) and (4) converge strongly in $H^1(\Omega)$ to $u_D(T, \overline{\eta}_C)$ and $u_N(\phi, \overline{\eta}_C)$ respectively.

(iii) Let ε, and M be two positive real numbers such that $\varepsilon < M$. For any $(\delta, \gamma) \in \mathbb{R}_+ \times \mathbb{R}_+^*$ and $\alpha \in [\varepsilon, M]$:

$$\|\overline{\eta}_D^{\delta,\alpha} - \overline{\eta}_C\|_{\widehat{H}^{\frac{1}{2}}(\Gamma_i)} + \|\overline{\eta}_N^{\delta,\alpha} - \overline{\eta}_C\|_{\widehat{H}^{\frac{1}{2}}(\Gamma_i)} \lesssim \ell(\delta, \gamma, \alpha) + \sqrt{\alpha}\left(\|\omega_D\|_{\widehat{H}^{-\frac{1}{2}}(\Gamma_c)} + \|\omega_N\|_{\widehat{H}^{\frac{1}{2}}(\Gamma_c)}\right), \tag{24a}$$

$$\|u_D(T^\delta, \overline{\eta}_D^{\delta,\alpha}) - u_D(T, \overline{\eta}_C)\|_{H^1(\Omega)} \lesssim \ell(\delta, \gamma, \alpha) + \sqrt{\alpha}\left(\|\omega_D\|_{\widehat{H}^{-\frac{1}{2}}(\Gamma_c)} + \|\omega_N\|_{\widehat{H}^{\frac{1}{2}}(\Gamma_c)}\right) + \delta, \tag{24b}$$

$$\|u_N(\phi^\delta, \overline{\eta}_N^{\delta,\alpha}) - u_N(\phi, \overline{\eta}_C)\|_{H^1(\Omega)} \lesssim \ell(\delta, \gamma, \alpha) + \sqrt{\alpha}\left(\|\omega_D\|_{\widehat{H}^{-\frac{1}{2}}(\Gamma_c)} + \|\omega_N\|_{\widehat{H}^{\frac{1}{2}}(\Gamma_c)}\right) + \delta. \tag{24c}$$

Proof. We first prove (i) and (ii): Using Proposition 5, it suffices to show that the regularized equilibrium $(\overline{\eta}_D^\alpha, \overline{\eta}_N^\alpha)$ converges strongly to $(\overline{\eta}_C, \overline{\eta}_C)$ as $\alpha \to 0$, and that the corresponding solutions converge strongly to the exact solution. Consider the regularized combined cost functional:

$$\begin{aligned} L^{\gamma,\alpha}(\eta_D, \eta_N) = \frac{1}{2}\|\lambda_D^c(T, \eta_D) - \phi\|^2_{H^{-\frac{1}{2}}(\Gamma_c)} + \frac{1}{2}\|u_N(\phi, \eta_N) - T\|^2_{\widehat{H}^{\frac{1}{2}}(\Gamma_c)} \\ + \frac{\gamma}{2}\|\lambda_D^i(T, \eta_D) - \lambda_N^i(\phi, \eta_N)\|^2_{H^{-\frac{1}{2}}(\Gamma_i)} + \frac{\alpha}{2}\|\eta_D\|^2_{H^{\frac{1}{2}}(\Gamma_i)} + \frac{\alpha}{2}\|\eta_N\|^2_{H^{\frac{1}{2}}(\Gamma_i)}. \end{aligned}$$

Let $\overline{\eta}_C = \overline{v}|_{\Gamma_i}$ be the exact boundary trace. Since the exact solution satisfies the Cauchy problem, we have:

$$L^{\gamma,\alpha}(\overline{\eta}_C, \overline{\eta}_C) = \alpha\|\overline{\eta}_C\|^2_{H^{\frac{1}{2}}(\Gamma_i)}.$$

By the minimizing property of the Nash equilibrium:

$$\frac{\alpha}{2}\|\overline{\eta}_D^\alpha\|^2_{H^{\frac{1}{2}}(\Gamma_i)} + \frac{\alpha}{2}\|\overline{\eta}_N^\alpha\|^2_{H^{\frac{1}{2}}(\Gamma_i)} \leq L^{\gamma,\alpha}(\overline{\eta}_D^\alpha, \overline{\eta}_N^\alpha) \leq \alpha\|\overline{\eta}_C\|^2_{H^{\frac{1}{2}}(\Gamma_i)}. \tag{25}$$

This shows that the sequences $(\overline{\eta}_D^\alpha)$ and $(\overline{\eta}_N^\alpha)$ are uniformly bounded in $H^{\frac{1}{2}}(\Gamma_i)$ independently of α and γ. Therefore, there exist weak limits $\overline{\eta}_D^0$ and $\overline{\eta}_N^0$ such that:

$$\overline{\eta}_D^\alpha \rightharpoonup \overline{\eta}_D^0, \quad \overline{\eta}_N^\alpha \rightharpoonup \overline{\eta}_N^0 \quad \text{in } H^{\frac{1}{2}}(\Gamma_i) \text{ as } \alpha \to 0.$$

From the hybrid variational formulations (3)–(4), the associated solutions converge weakly to the solutions corresponding to the limits. Passing to the limit $\alpha \to 0$ in (25), we obtain:

$$\lambda_D^c(T, \overline{\eta}_D^\alpha) \to \phi \quad \text{in } H^{-\frac{1}{2}}(\Gamma_c), \quad u_N(\phi, \overline{\eta}_N^\alpha) \to T \quad \text{in } \widehat{H}^{\frac{1}{2}}(\Gamma_c).$$

Hence, the weak limits satisfy:

$$\lambda_D^c(T, \overline{\eta}_D^0) = \phi, \quad u_D(T, \overline{\eta}_D^0) = T \quad \text{on } \Gamma_c,$$

and similarly:

$$u_N(\phi, \overline{\eta}_N^0) = T, \quad \partial_n u_N(\phi, \overline{\eta}_N^0) = \phi \quad \text{on } \Gamma_c.$$

By uniqueness of the data completion problem:

$$\overline{\eta}_D^0 = \overline{\eta}_N^0 = \overline{\eta}_C, \quad u_D(T, \overline{\eta}_D^0) = u_N(\phi, \overline{\eta}_N^0) = \overline{v}.$$

To prove strong convergence, we use the variational formulations (3) and (4) to obtain:

$$\begin{aligned} \|u_D(T, \overline{\eta}_D^\alpha) - u_N(\phi, \overline{\eta}_N^\alpha)\|^2_{H^1(\Omega)} = \langle \lambda_D^i(T, \overline{\eta}_D^\alpha) - \lambda_N^i(\phi, \overline{\eta}_N^\alpha), u_D(T, \overline{\eta}_D^\alpha) - u_N(\phi, \overline{\eta}_N^\alpha) \rangle_{\Gamma_i} \\ + \langle \lambda_D^c(T, \overline{\eta}_D^\alpha) - \phi, u_D(T, \overline{\eta}_D^\alpha) - u_N(\phi, \overline{\eta}_N^\alpha) \rangle_{\Gamma_c}. \end{aligned}$$

From the Cauchy–Schwarz inequality and the continuity of the trace operator, it follows that

$$\|u_D(T, \overline{\eta}_D^\alpha) - u_N(\phi, \overline{\eta}_N^\alpha)\|_{H^1(\Omega)} \lesssim \|\lambda_D^i(T, \overline{\eta}_D^\alpha) - \lambda_N^i(\phi, \overline{\eta}_N^\alpha)\|_{H^{-\frac{1}{2}}(\Gamma_i)} + \|\lambda_D^c(T, \overline{\eta}_D^\alpha) - \phi\|_{H^{-\frac{1}{2}}(\Gamma_c)}. \tag{26}$$

Since $L^{\gamma,\alpha}(\overline{\eta}_D^\alpha, \overline{\eta}_N^\alpha) \to 0$ as $\alpha \to 0$, the right-hand side of (26) tends to 0. Thus:

$$u_D(T, \overline{\eta}_D^\alpha) - u_N(\phi, \overline{\eta}_N^\alpha) \to 0 \quad \text{strongly in } H^1(\Omega).$$

By continuity of the trace operator:

$$\overline{\eta}_D^\alpha - \overline{\eta}_N^\alpha \to 0 \quad \text{strongly in } \widehat{H}^{\frac{1}{2}}(\Gamma_i).$$

Since both sequences converge weakly to $\overline{\eta}_C$, inequality (25) together with the parallelogram identity, directly implies that both sequences converge strongly to $\overline{\eta}_C$. Consequently, the corresponding solutions converge strongly in $H^1(\Omega)$ to the exact solution. This completes the proof of (i) and (ii). Now we come to proving (iii): By combining the stability estimates in Proposition 5 with the regularization error bounds from Proposition 4 via the triangle inequality:

$$\begin{aligned} \|\overline{\eta}_D^{\delta,\alpha} - \overline{\eta}_C\| &\leq \|\overline{\eta}_D^{\delta,\alpha} - \overline{\eta}_D^\alpha\| + \|\overline{\eta}_D^\alpha - \overline{\eta}_C\| \\ &\lesssim \ell(\delta, \gamma, \alpha) + \sqrt{\alpha} \left(\|\omega_D\|_{\widehat{H}^{-\frac{1}{2}}(\Gamma_c)} + \|\omega_N\|_{\widehat{H}^{\frac{1}{2}}(\Gamma_c)} \right), \end{aligned}$$

and similarly for $\overline{\eta}_N^{\delta,\alpha}$ which gives (24a). The solution error estimates (24b)-(24c) follow analogously. □

Proposition 7 (Optimal Error Bound Rate)**.** *Under the assumptions of Proposition 6, the optimal parameter choice that minimizes the convergence rate is:*

$$\alpha_{opt} = \sqrt{2}\delta, \quad \gamma_{opt} = (2)^{1/4} \sqrt{\delta}.$$

With this choice, the following optimal Error Bound rates are achieved:

$$\begin{aligned}\|\overline{\eta}_D^{\delta,\alpha_{opt}} - \overline{\eta}_D\|_{\widehat{H}^{\frac{1}{2}}(\Gamma_i)} + \|\overline{\eta}_N^{\delta,\alpha_{opt}} - \overline{\eta}_N\|_{\widehat{H}^{\frac{1}{2}}(\Gamma_i)} &\lesssim \delta^{1/2},\\ \|u_D(T^\delta, \overline{\eta}_D^{\delta,\alpha_{opt}}) - u_D(T, \overline{\eta}_D)\|_{H^1(\Omega)} &\lesssim \delta^{1/2},\\ \|u_N(\phi^\delta, \overline{\eta}_N^{\delta,\alpha_{opt}}) - u_N(\phi, \overline{\eta}_N)\|_{H^1(\Omega)} &\lesssim \delta^{1/2}.\end{aligned}$$

The rate $\delta^{1/2}$ is the balanced rate predicted by the present error bound when the parameters are chosen so as to equilibrate the noise amplification, regularization, and coupling terms.

Proof. Consider the general error bound:

$$E(\alpha, \gamma) = \sqrt{\frac{\delta^2}{\alpha} + \frac{\gamma^2\delta^2}{\alpha^2}} + \sqrt{\alpha} + \delta.$$

To minimize the dominant terms, we balance the competing errors:

- Noise amplification: $\delta/\sqrt{\alpha}$ and $\gamma\delta/\alpha$
- Approximation error: $\sqrt{\alpha}$

Setting $\gamma = \sqrt{\alpha}$ eliminates the γ-dependence in the balance:

$$E(\alpha) = \sqrt{\frac{2\delta^2}{\alpha}} + \sqrt{\alpha} + \delta.$$

Minimizing $\sqrt{\frac{2\delta^2}{\alpha}} + \sqrt{\alpha}$ gives:

$$\frac{d}{d\alpha}\left(\sqrt{\frac{2\delta^2}{\alpha}} + \sqrt{\alpha}\right) = -\frac{\sqrt{2}\delta}{2\alpha^{3/2}} + \frac{1}{2\sqrt{\alpha}} = 0.$$

Solving yields:

$$\frac{\sqrt{2}\delta}{2\alpha^{3/2}} = \frac{1}{2\sqrt{\alpha}} \Rightarrow \sqrt{2}\delta = \alpha \Rightarrow \alpha_{\text{opt}} = \sqrt{2}\delta,$$

and thus $\gamma_{\text{opt}} = \sqrt{\alpha_{\text{opt}}} = (2)^{1/4}\sqrt{\delta}$. Substituting back:

$$E(\sqrt{2}\delta, (2)^{1/4}\sqrt{\delta}) = (2)^{5/4}\sqrt{\delta} \lesssim \sqrt{\delta}.$$

The optimality follows from the fact that this choice balances the noise amplification and regularization errors at the same order $\delta^{1/2}$. □

Remark 1. The proof of Proposition 6 builds upon the framework established in [3]. The error between regularized solutions with noisy data and the exact solution exhibits the error bound rate:

$$\mathcal{O}\left(\frac{\delta}{\sqrt{\alpha}} + \sqrt{\alpha} + \frac{\gamma\delta}{\alpha}\right) \quad \text{for all } \alpha \in [\varepsilon, M].$$

This rate emerges from balancing three distinct error components: approximation error, noise propagation, and coupling effects between the Dirichlet and Neumann players.

Remark 2. A notable advantage of our approach is that the error bound rate is obtained under the baseline assumption that the missing data $\overline{\eta}_C$ belongs to $H^{\frac{1}{2}}(\Gamma_i)$, together with the restriction $\alpha \in [\varepsilon, M]$, and without imposing additional source-type conditions on the exact solution. This stands in contrast with classical Tikhonov regularization [49], which typically relies on such assumptions to derive comparable error estimates. The counterpart of this flexibility is that the inequalities (24a), (24b) and (24c), established uniformly on a fixed admissible interval of regularization parameters, are not intended, by themselves, to yield a direct convergence result as the regularization parameter tends to zero.

Remark 3. The restriction $\alpha \in [\varepsilon, M]$ with $0 < \varepsilon < M$ is well-justified in practical applications. The error estimate involves three competing terms: $\sqrt{\alpha}$ representing approximation error, $\delta/\sqrt{\alpha}$ capturing noise amplification, and $\gamma\delta/\alpha$ reflecting the coupling effect between players. The natural balance condition $\alpha > \delta^2$ emerges to maintain control over all three terms simultaneously, ensuring the total error remains bounded and decays appropriately.

Remark 4. The estimates in Proposition 6 highlight the essential role of regularization. When $\alpha = 0$, the right-hand sides of (24a)–(24c) become unbounded, demonstrating that quantitative error bounds require $\alpha > 0$. Without regularization, one can only establish qualitative stability through strong convergence results, but cannot obtain explicit error bound rates.

3 Finite Element Discretization

This section presents the discretized formulation of the Nash equilibrium problem (6), (10) using standard conforming finite element method based on polynomials of degree $k \geq 1$ [17].

3.1 Discrete Game Formulation

Let $\mathcal{T}^h$ be a quasi-uniform triangulation of the domain Ω with mesh size parameter $h > 0$, satisfying $\overline{\Omega} = \bigcup_{K \in \mathcal{T}^h} K$. We consider the following finite element spaces:

$$
\begin{aligned}
V^h &= \left\{ v^h \in C^0(\overline{\Omega}) : v^h|_T \ \in \mathbb{P}_k(T),\ \forall T \in \mathcal{T}^h \right\}, \\
W^h &= \left\{ v^h \in L^2(\overline{\Omega}) : v^h|_T \ \in \mathbb{P}_k(T),\ \forall T \in \mathcal{T}^h \right\}, \\
V^h_\Gamma &= V^h|_\Gamma \ \subset H^{\frac{1}{2}}(\Gamma), \quad M^h_{\Gamma_k} = W^h|_{\Gamma_k} \subset H^{-\frac{1}{2}}(\Gamma_k), \quad \text{for } k \in \{i, c\}, \\
\widehat{H}^{h\frac{1}{2}}(\Gamma_k) &= \left\{ v^h = \tilde{v}^h|_{\Gamma_k} : \tilde{v}^h \in V^h_\Gamma,\ \mathrm{supp}(\tilde{v}^h) \subset \Gamma_k \right\} \subset \widehat{H}^{\frac{1}{2}}(\Gamma_k).
\end{aligned}
$$

Let $\Pi^h_{\widehat{H}^{h\frac{1}{2}}(\Gamma_c)}$ be the standard Lagrange interpolation operator onto $\widehat{H}^{h\frac{1}{2}}(\Gamma_c)$ and $\pi^h_{M^h_{\Gamma_c}}$ be the L^2-projection operator onto $M^h_{\Gamma_c}$. The discrete counterparts of the data are denoted by T_h, ϕ_h for exact data and T^δ_h, ϕ^δ_h for noisy data, obtained by applying the corresponding projection operators. We recall that for all $\phi \in H^m(\Gamma_c)$ and $T \in H^{m+1}(\Gamma_c)$ with $1 \leq m \leq k+1$, the following interpolation error estimates hold [17, 23]:

$$
\|\phi - \pi^h_{M^h_{\Gamma_c}} \phi\|_{H^{-\frac{1}{2}}(\Gamma_c)} \lesssim h^{m+\frac{1}{2}} \|\phi\|_{H^m(\Gamma_c)}, \tag{28}
$$

$$
\|T - \Pi^h_{\widehat{H}^{h\frac{1}{2}}(\Gamma_c)} T\|_{H^{\frac{1}{2}}(\Gamma_c)} \lesssim h^{m+\frac{1}{2}} \|T\|_{H^{m+1}(\Gamma_c)}. \tag{29}
$$

In the discrete setting, state and control variables are restricted to the finite-dimensional spaces defined previously. To avoid unnecessary technical complications and to focus on the intrinsic

difficulties of the data completion problem, the solutions of the direct problems (3) and (4) are computed exactly. Consequently, the convergence analysis and error estimates depend additionally on the mesh size h and the polynomial degree k. For any $(\eta_{Dh}, \eta_{Nh}) \in (\widehat{H}^{\frac{1}{2}}(\Gamma_i))^2$, the discrete cost functionals are defined as follows:

$$H_{Dh}^{\gamma,\alpha}(\eta_{Dh}, \eta_{Nh}) = \frac{1}{2} a_D^{\alpha,\gamma}(\eta_{Dh}, \eta_{Dh}) - l_{Dh,\eta_{Nh}}^{\gamma}(\eta_{Dh}) + d_{Dh,\eta_{Nh}}^{\gamma}, \tag{30a}$$

$$H_{Nh}^{\gamma,\alpha}(\eta_{Dh}, \eta_{Nh}) = \frac{1}{2} a_N^{\alpha,\gamma}(\eta_{Nh}, \eta_{Nh}) - l_{Nh,\eta_{Dh}}^{\gamma}(\eta_{Nh}) + d_{N,\eta_{Dh}}^{\gamma}, \tag{30b}$$

$$H_{Dh}^{\gamma,\delta,\alpha}(\eta_{Dh}, \eta_{Nh}) = \frac{1}{2} a_D^{\alpha,\gamma}(\eta_{Dh}, \eta_{Dh}) - l_{Dh,\eta_{Nh}}^{\delta,\gamma}(\eta_{Dh}) + d_{Dh,\eta_{Nh}}^{\delta}, \tag{30c}$$

$$H_{Nh}^{\gamma,\delta,\alpha}(\eta_{Dh}, \eta_{Nh}) = \frac{1}{2} a_N^{\alpha,\gamma}(\eta_{Nh}, \eta_{Nh}) - l_{Nh,\eta_{Dh}}^{\delta,\gamma}(\eta_{Nh}) + d_{N,\eta_{Dh}}^{\delta}, \tag{30d}$$

where the linear forms and constant terms are defined analogously to the continuous case in Section 1.2, with (T, ϕ) replaced by (T_h, ϕ_h) or $(T_h^\delta, \phi_h^\delta)$ as appropriate.

Definition 3. *A pair* $(\overline{\eta}_{Dh}^{\alpha}, \overline{\eta}_{Nh}^{\alpha}) \in (\widehat{H}^{h\frac{1}{2}}(\Gamma_i))^2$ *is a* discrete regularized Nash equilibrium *(drNE) if*

$$\begin{cases} H_{Dh}^{\gamma,\alpha}(\overline{\eta}_{Dh}^{\alpha}, \overline{\eta}_{Nh}^{\alpha}) \leq H_{Dh}^{\gamma,\alpha}(\eta, \overline{\eta}_{Nh}^{\alpha}), & \forall \eta \in \widehat{H}^{h\frac{1}{2}}(\Gamma_i), \\ H_{Nh}^{\gamma,\alpha}(\overline{\eta}_{Dh}^{\alpha}, \overline{\eta}_{Nh}^{\alpha}) \leq H_{N}^{\gamma,\alpha}(\overline{\eta}_{Dh}^{\alpha}, \eta), & \forall \eta \in \widehat{H}^{h\frac{1}{2}}(\Gamma_i). \end{cases} \tag{31}$$

A pair $(\overline{\eta}_{Dh}^{\delta,\alpha}, \overline{\eta}_{Nh}^{\delta,\alpha}) \in (\widehat{H}^{h\frac{1}{2}}(\Gamma_i))^2$ *is a* discrete noisy Nash equilibrium *(dnNE) if*

$$\begin{cases} H_{Dh}^{\gamma,\delta,\alpha}(\overline{\eta}_{Dh}^{\delta,\alpha}, \overline{\eta}_{Nh}^{\delta,\alpha}) \leq H_{Dh}^{\gamma,\delta,\alpha}(\eta, \overline{\eta}_{Nh}^{\delta,\alpha}), & \forall \eta \in \widehat{H}^{h\frac{1}{2}}(\Gamma_i), \\ H_{Nh}^{\gamma,\delta,\alpha}(\overline{\eta}_{Dh}^{\delta,\alpha}, \overline{\eta}_{Nh}^{\delta,\alpha}) \leq H_{Nh}^{\gamma,\delta,\alpha}(\overline{\eta}_{Dh}^{\delta,\alpha}, \eta), & \forall \eta \in \widehat{H}^{h\frac{1}{2}}(\Gamma_i). \end{cases} \tag{32}$$

Proposition 8. *The partial mappings* $\eta_{Dh} \longmapsto H_{Dh}^{\gamma,\delta,\alpha}(\eta_{Dh}, \eta_N)$ *and* $\eta_{Nh} \longmapsto H_{Nh}^{\gamma,\delta,\alpha}(\eta_{Dh}, \eta_{Nh})$ *are twice differentiable, quadratic, and* α*-strongly convex functionals over* $\widehat{H}^{h\frac{1}{2}}(\Gamma_i)$.

Proof. The proof follows the same structure as Proposition 1 in the continuous setting. □

3.2 Stability and Error Estimates

The stability estimates from Proposition 5 extend to the discrete setting for both Nash equilibria defined in Definition 3, under the discrete noise bound:

$$\|T_h - T_h^\delta\|^2_{\widehat{H}^{\frac{1}{2}}(\Gamma_c)} + \|\phi_h - \phi_h^\delta\|^2_{H^{-\frac{1}{2}}(\Gamma_c)} \leq \delta^2. \tag{33}$$

Proposition 9 (Stability of Discrete Nash Equilibrium)**.** *There exists a unique discrete regularized Nash equilibrium* $(\overline{\eta}_{Dh}^{\alpha}, \overline{\eta}_{Nh}^{\alpha})$ *for parameters* $(\alpha, \gamma) \in (\mathbb{R}_+^*)^2$*, defined by (30a), (30b) and (31). Similarly, there exists a unique discrete noisy regularized Nash equilibrium* $(\overline{\eta}_{Dh}^{\delta,\alpha}, \overline{\eta}_{Nh}^{\delta,\alpha})$ *for parameters* $(\delta, \alpha, \gamma) \in \mathbb{R}_+ \times (\mathbb{R}_+^*)^2$ *defined by (30c), (30d) and (32), which strongly converges to* $(\overline{\eta}_{Dh}^{\alpha}, \overline{\eta}_{Nh}^{\alpha})$ *as* $\delta \to 0$*. Furthermore we have:*

$$\begin{aligned} &\|\overline{\eta}_{Dh}^{\delta,\alpha} - \overline{\eta}_{Dh}^{\alpha}\|_{\widehat{H}^{\frac{1}{2xce}}(\Gamma_i)} + \|\overline{\eta}_{Nh}^{\delta,\alpha} - \overline{\eta}_{Nh}^{\alpha}\|_{\widehat{H}^{\frac{1}{2}}(\Gamma_i)} \lesssim \ell(\delta, \gamma, \alpha), \\ &\|u_{hD}(T_h^\delta, \overline{\eta}_{Dh}^{\delta,\alpha}) - u_{hD}(T_h^\delta, \overline{\eta}_{Dh}^{\alpha})\|_{H^1(\Omega)} \lesssim \ell(\delta, \gamma, \alpha) + \delta, \\ &\|u_N(\phi^\delta, \overline{\eta}_{Nh}^{\delta,\alpha}) - u_N(\phi^\delta, \overline{\eta}_{Nh}^{\alpha})\|_{H^1(\Omega)} \lesssim \ell(\delta, \gamma, \alpha) + \delta, \end{aligned}$$

Proof. The proof is the same as Proposition 3 and Proposition 5. ■

Lemma 3 (FEM Error Bounds)**.** *Let $\overline{\eta}_D^\alpha$ and $\overline{\eta}_N^\alpha$ in $\widehat{H}^{s+\frac{1}{2}}(\Gamma_i)$ for $s \in [0,k]$, and consider parameters $(\delta,\alpha,\gamma) \in \mathbb{R}_+ \times (\mathbb{R}_+^*)^2$. Define $\widetilde{\eta}_{Dh}^\alpha$ and $\widetilde{\eta}_{Nh}^\alpha$ as the unique solutions to the discrete variational problems:*

$$a_D^{\alpha,\gamma}(\widetilde{\eta}_{Dh},\psi_h) = l^\gamma_{D,\overline{\eta}_N^\alpha}(\psi_h), \quad \forall \psi_h \in \widehat{H}^{h\frac{1}{2}}(\Gamma_i),$$
$$a_N^{\alpha,\gamma}(\widetilde{\eta}_{Nh},\psi_h) = l_{N,\overline{\eta}_D^\alpha}(\psi_h), \quad \forall \psi_h \in \widehat{H}^{h\frac{1}{2}}(\Gamma_i).$$

Then the following estimates hold:

$$\begin{aligned}\|\overline{\eta}_{Dh}^\alpha - \widetilde{\eta}_{Dh}^\alpha\|_{\widehat{H}^{\frac{1}{2}}(\Gamma_i)} + \|\overline{\eta}_{Nh}^\alpha - \widetilde{\eta}_{Nh}^\alpha\|_{\widehat{H}^{\frac{1}{2}}(\Gamma_i)} &\\ \lesssim \frac{1+\gamma}{\lambda_h^1+\alpha} h^s \left(\|T\|_{\widehat{H}^{s+\frac{1}{2}}(\Gamma_c)} + \|\phi\|_{\widehat{H}^{s-\frac{1}{2}}(\Gamma_c)}\right) &\\ + \frac{\gamma}{\lambda_h^1+\alpha}\left(\|\widetilde{\eta}_{Dh}^\alpha - \overline{\eta}_D^\alpha\|_{\widehat{H}^{\frac{1}{2}}(\Gamma_i)} + \|\widetilde{\eta}_{Nh}^\alpha - \overline{\eta}_N^\alpha\|_{\widehat{H}^{\frac{1}{2}}(\Gamma_i)}\right), &\quad (36)\end{aligned}$$

$$\|\widetilde{\eta}_{Dh}^\alpha - \overline{\eta}_D^\alpha\|_{\widehat{H}^{\frac{1}{2}}(\Gamma_i)} \lesssim \frac{1+\alpha+\gamma}{\lambda_{Dh}^1+\alpha} h^s \|\overline{\eta}_D^\alpha\|_{\widehat{H}^{s+\frac{1}{2}}(\Gamma_i)}, \quad (37)$$

$$\|\widetilde{\eta}_{Nh}^\alpha - \overline{\eta}_N^\alpha\|_{\widehat{H}^{\frac{1}{2}}(\Gamma_i)} \lesssim \frac{1+\alpha+\gamma}{\lambda_{Nh}^1+\alpha} h^s \|\overline{\eta}_N^\alpha\|_{\widehat{H}^{s+\frac{1}{2}}(\Gamma_i)}. \quad (38)$$

Here λ_{Dh}^1 denotes the smallest eigenvalue of the self-adjoint, positive definite operator $(S_D^h)^* S_D^h$, while λ_{Nh}^1 denotes the smallest eigenvalue of $(S_N^h)^* S_N^h$. The operators S_D^h and S_N^h are defined as follows:

$$S_D^h: \begin{array}{ccc} \widehat{H}^{h\frac{1}{2}}(\Gamma_i) & \longrightarrow & M_{\Gamma_c}^h \\ \eta_{Dh} & \longmapsto & S^h(\eta_{Dh}) = \lambda_D^c(0,\widetilde{\eta}_{Dh}), \end{array} \quad \text{and} \quad S_N^h: \begin{array}{ccc} \widehat{H}^{h\frac{1}{2}}(\Gamma_i) & \longrightarrow & \widehat{H}^{h\frac{1}{2}}(\Gamma_c) \\ \eta_{Nh} & \longmapsto & S^h(\eta_{Nh}) = u_N(0,\eta_{Nh})|_{\Gamma_v} \end{array}.$$

The operators $(S_D^h)^*$ and $(S_N^h)^*$ denote the adjoints of S_D^h and S_N^h. Also, we have $\lambda_1^h = \min(\lambda_{Dh}^1, \lambda_{Nh}^1)$.

Proof. We begin with the variational formulations:

$$a_D^{\alpha,\gamma}(\widetilde{\eta}_{Dh}^\alpha,\psi_h) = l^\gamma_{D,\overline{\eta}_N^\alpha}(\psi_h),$$
$$a_D^{\alpha,\gamma}(\overline{\eta}_{Dh}^\alpha,\psi_h) = l^\gamma_{D,\overline{\eta}_{Nh}^\alpha}(\psi_h),$$

for all $\psi_h \in \widehat{H}^{h\frac{1}{2}}(\Gamma_i)$. Subtracting the two equations and testing with $\psi_h = \overline{\eta}_{Dh}^\alpha - \widetilde{\eta}_{Dh}^\alpha$, then expanding the linear forms using their definitions:

$$\begin{aligned}a_D^{\alpha,\gamma}(\overline{\eta}_{Dh}^\alpha - \widetilde{\eta}_{Dh}^\alpha, \overline{\eta}_{Dh}^\alpha - \widetilde{\eta}_{Dh}^\alpha) &= -\int_{\Gamma_c} \lambda_D^c(0,\overline{\eta}_{Dh}^\alpha - \widetilde{\eta}_{Dh}^\alpha)\big(\lambda_D^c(T_h - T,0) - (\phi_h - \phi)\big)d\Gamma \\ &+ \gamma \int_{\Gamma_i} \lambda_D^i(0,\overline{\eta}_{Dh}^\alpha - \widetilde{\eta}_{Dh}^\alpha)\big(\lambda_D^i(T_h - T,0) - \lambda_N^i(\phi_h - \phi,0)\big)d\Gamma \\ &+ \gamma \int_{\Gamma_i} \lambda_D^i(0,\overline{\eta}_{Dh}^\alpha - \widetilde{\eta}_{Dh}^\alpha)\lambda_N^i(0,\overline{\eta}_N^\alpha - \overline{\eta}_{Nh}^\alpha)d\Gamma.\end{aligned}$$

We now estimate each term separately. For the first term, using Cauchy-Schwarz inequality and the continuity of the solution operators:

$$\begin{aligned}&\left|\int_{\Gamma_c} \lambda_D^c(0,\overline{\eta}_{Dh}^\alpha - \widetilde{\eta}_{Dh}^\alpha)\big(\lambda_D^c(T_h - T,0) - (\phi_h - \phi)\big)d\Gamma\right| \\ &\quad\lesssim \|\lambda_D^c(0,\overline{\eta}_{Dh}^\alpha - \widetilde{\eta}_{Dh}^\alpha)\|_{\widehat{H}^{-\frac{1}{2}}(\Gamma_c)} \\ &\qquad\times \left(\|\lambda_D^c(T_h - T,0)\|_{\widehat{H}^{-\frac{1}{2}}(\Gamma_c)} + \|\phi_h - \phi\|_{\widehat{H}^{-\frac{1}{2}}(\Gamma_c)}\right) \\ &\quad\lesssim \|\overline{\eta}_{Dh}^\alpha - \widetilde{\eta}_{Dh}^\alpha\|_{\widehat{H}^{\frac{1}{2}}(\Gamma_i)} \left(\|T_h - T\|_{\widehat{H}^{\frac{1}{2}}(\Gamma_c)} + \|\phi_h - \phi\|_{\widehat{H}^{-\frac{1}{2}}(\Gamma_c)}\right).\end{aligned}$$

For the second term:

$$\begin{aligned}&\left|\gamma\int_{\Gamma_i}\lambda_D^i(0,\overline{\eta}_{Dh}^\alpha-\widetilde{\eta}_{Dh}^\alpha)\big(\lambda_D^i(T_h-T,0)-\lambda_N^i(\phi_h-\phi,0)\big)d\Gamma\right|\\&\quad\lesssim\gamma\|\overline{\eta}_{Dh}^\alpha-\widetilde{\eta}_{Dh}^\alpha\|_{\widehat{H}^{\frac12}(\Gamma_i)}\left(\|T_h-T\|_{\widehat{H}^{\frac12}(\Gamma_c)}+\|\phi_h-\phi\|_{\widehat{H}^{-\frac12}(\Gamma_c)}\right).\end{aligned}$$

For the third term, using the triangle inequality and Young's inequality:

$$\begin{aligned}&\left|\gamma\int_{\Gamma_i}\lambda_D^i(0,\overline{\eta}_{Dh}^\alpha-\widetilde{\eta}_{Dh}^\alpha)\lambda_N^i(0,\overline{\eta}_N^\alpha-\overline{\eta}_{Nh}^\alpha)d\Gamma\right|\\&\quad\le\frac{\gamma}{2}\|\lambda_D^i(0,\overline{\eta}_{Dh}^\alpha-\widetilde{\eta}_{Dh}^\alpha)\|^2_{\widehat{H}^{-\frac12}(\Gamma_i)}+\frac{\gamma}{2}\|\lambda_N^i(0,\overline{\eta}_{Nh}^\alpha-\widetilde{\eta}_{Nh}^\alpha)\|^2_{\widehat{H}^{-\frac12}(\Gamma_i)}\\&\qquad+\gamma\|\lambda_D^i(0,\overline{\eta}_{Dh}^\alpha-\widetilde{\eta}_{Dh}^\alpha)\|_{\widehat{H}^{-\frac12}(\Gamma_i)}\|\lambda_N^i(0,\overline{\eta}_N^\alpha-\widetilde{\eta}_{Nh}^\alpha)\|_{\widehat{H}^{-\frac12}(\Gamma_i)}\end{aligned}$$

Combining all three estimates:

$$\begin{aligned}&a_D^{\alpha,\gamma}(\overline{\eta}_{Dh}^\alpha-\widetilde{\eta}_{Dh}^\alpha,\overline{\eta}_{Dh}^\alpha-\widetilde{\eta}_{Dh}^\alpha)-\frac{\gamma}{2}\|\lambda_D^i(0,\overline{\eta}_{Dh}^\alpha-\widetilde{\eta}_{Dh}^\alpha)\|^2_{\widehat{H}^{-\frac12}(\Gamma_i)}-\frac{\gamma}{2}\|\lambda_N^i(0,\overline{\eta}_{Nh}^\alpha-\widetilde{\eta}_{Nh}^\alpha)\|^2_{\widehat{H}^{-\frac12}(\Gamma_i)}\\&\lesssim(1+\gamma)\|\overline{\eta}_{Dh}^\alpha-\widetilde{\eta}_{Dh}^\alpha\|_{\widehat{H}^{\frac12}(\Gamma_i)}\left(\|T_h-T\|_{\widehat{H}^{\frac12}(\Gamma_c)}+\|\phi_h-\phi\|_{\widehat{H}^{-\frac12}(\Gamma_c)}\right)\\&\quad+\ \gamma\|\overline{\eta}_{Dh}^\alpha-\widetilde{\eta}_{Dh}^\alpha\|_{\widehat{H}^{\frac12}(\Gamma_i)}\|\overline{\eta}_N^\alpha-\widetilde{\eta}_{Nh}^\alpha\|_{\widehat{H}^{\frac12}(\Gamma_i)}.\end{aligned}$$

A similar analysis for the Neumann component yields:

$$\begin{aligned}&a_N^{\alpha,\gamma}(\overline{\eta}_{Nh}^\alpha-\widetilde{\eta}_{Nh}^\alpha,\overline{\eta}_{Nh}^\alpha-\widetilde{\eta}_{Nh}^\alpha)-\frac{\gamma}{2}\|\lambda_D^i(0,\overline{\eta}_{Dh}^\alpha-\widetilde{\eta}_{Dh}^\alpha)\|^2_{\widehat{H}^{-\frac12}(\Gamma_i)}-\frac{\gamma}{2}\|\lambda_N^i(0,\overline{\eta}_{Nh}^\alpha-\widetilde{\eta}_{Nh}^\alpha)\|^2_{\widehat{H}^{-\frac12}(\Gamma_i)}\\&\lesssim(1+\gamma)\|\overline{\eta}_{Nh}^\alpha-\widetilde{\eta}_{Nh}^\alpha\|_{\widehat{H}^{\frac12}(\Gamma_i)}\left(\|T_h-T\|_{\widehat{H}^{\frac12}(\Gamma_c)}+\|\phi_h-\phi\|_{\widehat{H}^{-\frac12}(\Gamma_c)}\right)\\&\quad+\ \gamma\|\overline{\eta}_{Nh}^\alpha-\widetilde{\eta}_{Nh}^\alpha\|_{\widehat{H}^{\frac12}(\Gamma_i)}\|\overline{\eta}_D^\alpha-\widetilde{\eta}_{Dh}^\alpha\|_{\widehat{H}^{\frac12}(\Gamma_i)}.\end{aligned}$$

Adding both inequalities and using the coercivity of the bilinear forms:

$$\begin{aligned}&(\lambda_h^1+\alpha)\left(\|\overline{\eta}_{Dh}^\alpha-\widetilde{\eta}_{Dh}^\alpha\|^2_{\widehat{H}^{\frac12}(\Gamma_i)}+\|\overline{\eta}_{Nh}^\alpha-\widetilde{\eta}_{Nh}^\alpha\|^2_{\widehat{H}^{\frac12}(\Gamma_i)}\right)\\&\lesssim(1+\gamma)\left(\|\overline{\eta}_{Dh}^\alpha-\widetilde{\eta}_{Dh}^\alpha\|_{\widehat{H}^{\frac12}(\Gamma_i)}+\|\overline{\eta}_{Nh}^\alpha-\widetilde{\eta}_{Nh}^\alpha\|_{\widehat{H}^{\frac12}(\Gamma_i)}\right)\\&\quad\times\left(\|T_h-T\|_{\widehat{H}^{\frac12}(\Gamma_c)}+\|\phi_h-\phi\|_{\widehat{H}^{-\frac12}(\Gamma_c)}\right)\\&\quad+\gamma\left(\|\widetilde{\eta}_{Dh}^\alpha-\overline{\eta}_D^\alpha\|^2_{\widehat{H}^{\frac12}(\Gamma_i)}+\|\widetilde{\eta}_{Nh}^\alpha-\overline{\eta}_N^\alpha\|^2_{\widehat{H}^{\frac12}(\Gamma_i)}\right).\end{aligned}$$

Using the interpolation estimates (28) and (29), we obtain the first inequality (36). For inequalities (37) and (38), we use Galerkin orthogonality:

$$\begin{aligned}a_D^{\alpha,\gamma}(\widetilde{\eta}_{Dh}^\alpha-\overline{\eta}_D^\alpha,\psi_h)=0,\quad\forall\psi_h\in\widehat{H}^{h\frac12}(\Gamma_i),\\a_N^{\alpha,\gamma}(\widetilde{\eta}_{Nh}^\alpha-\overline{\eta}_N^\alpha,\psi_h)=0,\quad\forall\psi_h\in\widehat{H}^{h\frac12}(\Gamma_i).\end{aligned}$$

Taking $\psi_{Dh} = \Pi^h_{\widehat{H}^{h\frac{1}{2}}(\Gamma_i)} \overline{\eta}^\alpha_D$ and using continuity:

$$\begin{aligned} a^{\alpha,\gamma}_D(\widetilde{\eta}^\alpha_{Dh} - \overline{\eta}^\alpha_D, \widetilde{\eta}^\alpha_{Dh} - \overline{\eta}^\alpha_D) &= a^{\alpha,\gamma}_D(\widetilde{\eta}^\alpha_{Dh} - \overline{\eta}^\alpha_D, \psi_{Dh} - \overline{\eta}^\alpha_D) \\ &\lesssim (1+\alpha+\gamma)\|\widetilde{\eta}^\alpha_{Dh} - \overline{\eta}^\alpha_D\|_{\widehat{H}^{\frac{1}{2}}(\Gamma_i)} \|\psi_{Dh} - \overline{\eta}^\alpha_D\|_{\widehat{H}^{\frac{1}{2}}(\Gamma_i)}. \end{aligned}$$

The coercivity of $a^{\alpha,\gamma}_D$ and standard interpolation estimates give:

$$(\lambda^1_{Dh} + \alpha)\|\widetilde{\eta}^\alpha_{Dh} - \overline{\eta}^\alpha_D\|_{\widehat{H}^{\frac{1}{2}}(\Gamma_i)} \lesssim (1+\alpha+\gamma) h^s \|\overline{\eta}^\alpha_D\|_{\widehat{H}^{s+\frac{1}{2}}(\Gamma_i)},$$

which proves (37). The estimate (38) follows similarly. □

Building on previous discrete stability and approximation results, we now establish the main error estimate for the Nash equilibrium in Definition 3, combining regularization error from the continuous setting with finite element discretization error.

Proposition 10 (A Priori Error Estimates)**.** *Let $\overline{v}$ be the exact solution of the continuous Cauchy problem for compatible data $(T,\phi) \in \widehat{H}^{\frac{1}{2}}(\Gamma_c) \times \widehat{H}^{-\frac{1}{2}}(\Gamma_c)$ such that $\overline{v} \in H^{s+1}(\Omega)$ and $\left(\overline{\eta}^\alpha_D, \overline{\eta}^\alpha_N\right) \in (\widehat{H}^{s+\frac{1}{2}}(\Gamma_i))^2$ with $0 \le s \le k$. Under the assumptions of Lemma 3 together with (33), the following estimates hold:*

$$\begin{aligned} &\|\overline{\eta}^{\delta,\alpha}_{Dh} - \overline{\eta}_C\|_{\widehat{H}^{\frac{1}{2}}(\Gamma_i)} + \|\overline{\eta}^{\delta,\alpha}_{Nh} - \overline{\eta}_C\|_{\widehat{H}^{\frac{1}{2}}(\Gamma_i)} \\ &\qquad \lesssim \ell(\delta,\gamma,\alpha) + \sqrt{\alpha} \\ &\qquad\quad + \frac{1+\gamma}{\lambda^1_h + \alpha} h^s \left(\|T\|_{\widehat{H}^{s+\frac{1}{2}}(\Gamma_c)} + \|\phi\|_{\widehat{H}^{s-\frac{1}{2}}(\Gamma_c)} \right) \\ &\qquad\quad + \frac{(1+\alpha+\gamma)\gamma}{(\lambda^1_h + \alpha)^2} h^s \left(\|\overline{\eta}^\alpha_D\|_{\widehat{H}^{s+\frac{1}{2}}(\Gamma_i)} + \|\overline{\eta}^\alpha_N\|_{\widehat{H}^{s+\frac{1}{2}}(\Gamma_i)} \right), \end{aligned} \tag{39a}$$

$$\|u_D(T^\delta_h, \overline{\eta}^{\delta,\alpha}_{Dh}) - \overline{v}\|_{H^1(\Omega)} \lesssim \delta + h^s \|T\|_{\widehat{H}^{s+\frac{1}{2}}(\Gamma_c)} + \|\overline{\eta}^{\delta,\alpha}_{Dh} - \overline{\eta}_C\|_{\widehat{H}^{\frac{1}{2}}(\Gamma_i)}, \tag{39b}$$

$$\|u_N(\phi^\delta_h, \overline{\eta}^{\delta,\alpha}_{Nh}) - \overline{v}\|_{H^1(\Omega)} \lesssim \delta + h^s \|\phi\|_{\widehat{H}^{s-\frac{1}{2}}(\Gamma_c)} + \|\overline{\eta}^{\delta,\alpha}_{Nh} - \overline{\eta}_C\|_{\widehat{H}^{\frac{1}{2}}(\Gamma_i)}. \tag{39c}$$

Proof. Using the triangular inequality, we have:

$$\begin{aligned} \|\overline{\eta}^{\delta,\alpha}_{Dh} - \overline{\eta}_C\|_{\widehat{H}^{\frac{1}{2}}(\Gamma_i)} \le\ & \|\overline{\eta}^{\delta,\alpha}_{Dh} - \overline{\eta}^\alpha_{Dh}\|_{\widehat{H}^{\frac{1}{2}}(\Gamma_i)} + \|\overline{\eta}^\alpha_{Dh} - \widetilde{\eta}^\alpha_{Dh}\|_{\widehat{H}^{\frac{1}{2}}(\Gamma_i)} \\ & + \|\widetilde{\eta}^\alpha_{Dh} - \overline{\eta}^\alpha_D\|_{\widehat{H}^{\frac{1}{2}}(\Gamma_i)} + \|\widetilde{\eta}^\alpha_D - \overline{\eta}_C\|_{\widehat{H}^{\frac{1}{2}}(\Gamma_i)} \end{aligned} \tag{40}$$

$$\begin{aligned} \|\overline{\eta}^{\delta,\alpha}_{Nh} - \overline{\eta}_C\|_{\widehat{H}^{\frac{1}{2}}(\Gamma_i)} \le\ & \|\overline{\eta}^{\delta,\alpha}_{Nh} - \overline{\eta}^\alpha_{Nh}\|_{\widehat{H}^{\frac{1}{2}}(\Gamma_i)} + \|\overline{\eta}^\alpha_{Nh} - \widetilde{\eta}^\alpha_{Nh}\|_{\widehat{H}^{\frac{1}{2}}(\Gamma_i)} \\ & + \|\widetilde{\eta}^\alpha_{Nh} - \overline{\eta}^\alpha_N\|_{\widehat{H}^{\frac{1}{2}}(\Gamma_i)} + \|\widetilde{\eta}^\alpha_N - \overline{\eta}_C\|_{\widehat{H}^{\frac{1}{2}}(\Gamma_i)} \end{aligned} \tag{41}$$

The first estimate (39a) is obtained by combining inequalities (40) and (41), the stability estimates from Lemma 3 and Proposition 9. For the second estimate (39b) and third estimate (39c), we use the triangle inequality:

$$\begin{aligned} \|u_D(T^\delta_h, \overline{\eta}^{\delta,\alpha}_{Dh}) - \overline{v}\|_{H^1(\Omega)} &\lesssim \|u_D(T^\delta_h - T_h, 0)\|_{H^1(\Omega)} + \|u_D(T_h - T, 0)\|_{H^1(\Omega)} \\ &\quad + \|u_D(0, \overline{\eta}^{\delta,\alpha}_{Dh} - \overline{\eta}_C)\|_{H^1(\Omega)} \\ &\lesssim \delta + h^s \|T\|_{\widehat{H}^{s+\frac{1}{2}}(\Gamma_c)} + \|\overline{\eta}^{\delta,\alpha}_{Dh} - \overline{\eta}_C\|_{\widehat{H}^{\frac{1}{2}}(\Gamma_i)}, \end{aligned}$$

and

$$\begin{aligned}\|u_N(\phi_h^\delta, \overline{\eta}_{Nh}^{\delta,\alpha}) - \overline{v}\|_{H^1(\Omega)} &\lesssim \|u_N(\phi_h^\delta - \phi_h, 0)\|_{H^1(\Omega)} + \|u_N(\phi_h - \phi, 0)\|_{H^1(\Omega)} \\ &\quad + \|u_N(0, \overline{\eta}_{Nh}^{\delta,\alpha} - \overline{\eta}_C)\|_{H^1(\Omega)} \\ &\lesssim \delta + h^s \|\phi\|_{\widehat{H}^{s-\frac{1}{2}}(\Gamma_c)} + \|\overline{\eta}_{Nh}^{\delta,\alpha} - \overline{\eta}_C\|_{\widehat{H}^{\frac{1}{2}}(\Gamma_i)},\end{aligned}$$

which completes the proof. □

Remark 1 (On the optimal error bound rate)**.** *According to Proposition 10, for regular data (e.g., $\delta \leq \alpha = h^r$ with $r \geq 1$), using a finite element method of order k and choosing $\gamma = \alpha$, the a priori error estimate for the missing data is:*

$$\|\overline{\eta}_{Dh}^{\delta,\alpha} - \overline{\eta}_C\| + \|\overline{\eta}_{Nh}^{\delta,\alpha} - \overline{\eta}_C\| \lesssim h^{\frac{r}{2}} + h^{s-r} \lesssim h^{\min\left(\frac{r}{2}, s-r\right)},$$

for all $0 \leq s \leq k$, $r \geq 0$. This implies that the optimal convergence rate for this parameter choice is $\mathcal{O}(h^{\frac{s}{3}})$, achieved when $r = \frac{2}{3}s$.

4 Numerical Implementation

4.1 Alternating Minimization Algorithm

To compute the Nash equilibrium, we employ an alternating minimization procedure following [6]:

$$\left|\begin{array}{l}\text{Given an initial state } (\overline{\eta}_{Dh}^0, \overline{\eta}_{Nh}^0), \text{ compute for all } k \geq 0: \\ \quad \overline{\eta}_{Dh}^{k+1} = \underset{\eta \in \widehat{H}^{h\frac{1}{2}}(\Gamma_i)}{\arg\min}\ H_{Dh}^{\delta,\alpha}(\eta, \overline{\eta}_{Nh}^k), \\ \quad \overline{\eta}_{Nh}^{k+1} = \underset{\eta \in \widehat{H}^{h\frac{1}{2}}(\Gamma_i)}{\arg\min}\ H_{Nh}^{\delta,\alpha}(\overline{\eta}_{Dh}^{k+1}, \eta).\end{array}\right.$$

The convergence of this alternating procedure is established in [6] under suitable assumptions that are satisfied in our framework.

4.2 Gradient Computation via Adjoint Method

At each iteration k, the optimization problems are solved using a gradient descent method. The gradients are computed efficiently via an adjoint state approach. For the Dirichlet player, we define the Lagrangian functional:

$$\begin{aligned}\mathcal{L}_D(\eta_D, \eta_N, u_D, v_D, \lambda_D^i, \mu_D^i, \lambda_D^c, \mu_D^c, \lambda_D^0, \mu_D^0) &= H_{Dh}^{\gamma,\delta,\alpha}(\eta_D, \eta_N) \\ &\quad + \int_\Omega \nabla u_D \cdot \nabla v_D d\Omega - \sum_{k \in \{i,c,0\}} \int_{\Gamma_k} \lambda_D^k v_D d\Gamma \\ &\quad - \sum_{k \in \{i,c,0\}} \int_{\Gamma_k} \mu_D^k (u_D - g_D^k) d\Gamma,\end{aligned}$$

where $g_D^i = \eta_D$, $g_D^c = T_h$, $g_D^0 = 0$. For the Neumann player, we have

$$\begin{aligned}\mathcal{L}_N(\eta_D, \eta_N, u_N, v_N, \lambda_N^i, \mu_N^i, \lambda_N^0, \mu_N^0) &= H_{Nh}^{\gamma,\delta,\alpha}(\eta_D, \eta_N) \\ &+ \int_\Omega \nabla u_N \cdot \nabla v_N d\Omega - \sum_{k\in\{i,0\}} \int_{\Gamma_k} \lambda_N^k v_N d\Gamma - \int_{\Gamma_c} \phi_h v_N d\Gamma \\ &- \sum_{k\in\{i,0\}} \int_{\Gamma_k} \mu_N^k (u_N - g_N^k) d\Gamma,\end{aligned}$$

where $g_N^i = \eta_N$, $g_N^0 = 0$. The state variables $(u_D, \lambda_D^i, \lambda_D^c, \lambda_D^0)$ satisfy the discrete Dirichlet problem:

$$\begin{cases} \text{Find } (u_D, \lambda_D^i, \lambda_D^c, \lambda_D^0) \in (V^h, M_{\Gamma_i}^h, M_{\Gamma_c}^h, M_{\Gamma_0}^h) \text{ such that:} \\ \displaystyle\int_\Omega \nabla u_D \cdot \nabla w_D d\Omega - \sum_{k\in\{i,c\}} \int_{\Gamma_k} \lambda_D^k w_D d\Gamma = 0, & \forall w_D \in V^h, \\ \displaystyle\int_{\Gamma_k} h_D^k (u_D - g_D^k) d\Gamma = 0, & \forall h_D^k \in M_{\Gamma_k}^h,\ k \in \{i, c, 0\}. \end{cases} \tag{42}$$

The state variables $(u_N, \lambda_N^i, \lambda_N^0)$ satisfy the discrete Neumann problem:

$$\begin{cases} \text{Find } (u_N, \lambda_N^i, \lambda_N^0) \in (V^h, M_{\Gamma_i}^h, M_{\Gamma_0}^h) \text{ such that:} \\ \displaystyle\int_\Omega \nabla u_N \cdot \nabla w_N d\Omega - \sum_{k\in\{i,0\}} \int_{\Gamma_k} \lambda_N^k w_N d\Gamma = \int_{\Gamma_c} \phi_h w_N d\Gamma, & \forall w_N \in V^h, \\ \displaystyle\int_{\Gamma_k} h_N^k (u_N - g_N^k) d\Gamma = 0, & \forall h_N^k \in M_{\Gamma_k}^h,\ k \in \{i, 0\}. \end{cases} \tag{43}$$

The gradients are then obtained as:

$$\begin{aligned} \frac{\partial H_{Dh}^{\gamma,\delta,\alpha}}{\partial \eta_D}(\eta_D, \eta_N) \cdot h_D^i &= \left(S_{ND}^i \mu_D^i + \alpha \eta_D, h_D^i\right)_{\widehat{H}^{h\frac{1}{2}}(\Gamma_i)}, \quad \forall h_D^i \in \widehat{H}^{h\frac{1}{2}}(\Gamma_i), \\ \frac{\partial H_{Nh}^{\gamma,\delta,\alpha}}{\partial \eta_N}(\eta_D, \eta_N) \cdot h_N^i &= \left(S_{ND}^i \mu_N^i + \alpha \eta_N, h_N^i\right)_{\widehat{H}^{h\frac{1}{2}}(\Gamma_i)}, \quad \forall h_N^i \in \widehat{H}^{h\frac{1}{2}}(\Gamma_i), \end{aligned}$$

where μ_D^i and μ_N^i are solutions of the adjoint problems. For the Dirichlet adjoint problem:

$$\begin{cases} \text{Find } (v_D, \mu_D^i, \mu_D^c, \mu_D^0) \in (V^h, M_{\Gamma_i}^h, M_{\Gamma_c}^h, M_{\Gamma_0}^h) \text{ such that:} \\ \displaystyle\int_\Omega \nabla v_D \cdot \nabla w_D d\Omega - \sum_{k\in\{i,c,0\}} \int_{\Gamma_k} \mu_D^k w_D d\Gamma = 0, & \forall w_D \in V^h, \\ \displaystyle\int_{\Gamma_i} h_D^i v_D d\Gamma + \gamma \left(h_D^i, \lambda_D^i - \lambda_N^i\right)_{H^{-\frac{1}{2}}(\Gamma_i)} = 0, & \forall h_D^i \in M_{\Gamma_i}^h, \\ \displaystyle\int_{\Gamma_c} h_D^c v_D d\Gamma + \left(h_D^c, \lambda_D^c - \phi_h\right)_{H^{-\frac{1}{2}}(\Gamma_c)} = 0, & \forall h_D^c \in M_{\Gamma_c}^h, \\ \displaystyle\int_{\Gamma_0} h_D^0 v_D d\Gamma = 0, & \forall h_D^0 \in M_{\Gamma_0}^h. \end{cases} \tag{44}$$

For the Neumann adjoint problem:

$$\begin{cases} \text{Find } (v_N, \mu_N^i, \mu_N^0) \in (V^h, M_{\Gamma_i}^h, M_{\Gamma_0}^h) \text{ such that:} \\ \displaystyle\int_\Omega \nabla v_N \cdot \nabla w_N d\Omega - \sum_{k\in\{i,0\}} \int_{\Gamma_k} \mu_N^k w_N d\Gamma + \left(u_N - T_h, w_N\right)_{H^{\frac{1}{2}}(\Gamma_c)} = 0, & \forall w_N \in V^h, \\ \displaystyle\int_{\Gamma_i} h_N^i v_N d\Gamma - \gamma \left(h_N^i, \lambda_D^i - \lambda_N^i\right)_{H^{-\frac{1}{2}}(\Gamma_i)} = 0, & \forall h_N^i \in M_{\Gamma_i}^h, \\ \displaystyle\int_{\Gamma_0} h_N^0 v_N d\Gamma = 0, & \forall h_N^0 \in M_{\Gamma_0}^h. \end{cases} \tag{45}$$

Remark 5. [Adjoint Systems] The adjoint problems admit the strong formulations:

$$\begin{cases} \text{Find } v_D \in H^1(\Omega) \text{ such that} \\ -\Delta v_D = 0 \quad \text{in } \Omega, \quad v_D|_{\Gamma_0} = 0 \\ v_D|_{\Gamma_c} = S_{ND}(\lambda_D^c - \phi_h), \\ v_D|_{\Gamma_i} = \gamma S_{ND}(\lambda_D^i - \lambda_N^i). \end{cases} \tag{A$_D$}$$

$$\begin{cases} \text{Find } v_N \in H^1(\Omega) \text{ such that} \\ -\Delta v_N = 0 \quad \text{in } \Omega, \quad v_N|_{\Gamma_0} = 0, \\ \partial_n v_N|_{\Gamma_c} = S_{ND}(u_N - T_h), \\ v_N|_{\Gamma_i} = -\gamma S_{ND}(\lambda_D^i - \lambda_N^i). \end{cases} \tag{A$_N$}$$

4.3 Computational Algorithm

The computation of the discrete Nash equilibrium is carried out using an alternating minimization algorithm, which implements the iterative scheme introduced in Equation (2). At each outer iteration, the two players update their strategies successively by solving their respective optimization subproblems while keeping the opponent's control fixed. To monitor convergence at both levels of the algorithm, we introduce two complementary error indicators. First, for each player, the inner-loop relative error quantifies the convergence of the gradient-based optimization process:

$$\varepsilon_* = \frac{|\eta_{*h}^{k+1,s+1} - \eta_{*h}^{k+1,s}|_{\widehat{H}^{\frac{1}{2}}(\Gamma_i)}}{|\eta_{*h}^{k+1,s}|_{\widehat{H}^{\frac{1}{2}}(\Gamma_i)}}, \quad * = D,\, N. \tag{46}$$

Second, the outer-loop Nash equilibrium residual

$$\varepsilon_{DN} = |\overline{\eta}_{Dh}^{k+1} - \overline{\eta}_{Nh}^{k+1}|_{\widehat{H}^{\frac{1}{2}}(\Gamma_i)}. \tag{47}$$

measures the consistency between the strategies of the two players and thus quantifies proximity to a Nash equilibrium.

Each player's optimization problem is solved using a gradient descent method, with gradients computed via the adjoint formulations described in Section 4.2. The inner-loop tolerance is fixed to $\varepsilon_{\text{inner}} = 10^{-2}$. This relatively loose threshold is sufficient during the early stages of the algorithm, where the mismatch between the players' strategies remains dominant and high precision in each subproblem is unnecessary. As the iterations proceed, the coupling term progressively enforces agreement between the Dirichlet and Neumann controls. Consequently, the algorithm naturally transitions from a classical best-response Nash iteration toward a more tightly coupled update mechanism. In this regime, the distinction between the two players' optimizations becomes less pronounced, and the algorithm effectively behaves as a one-shot inversion method [12, 50], where both controls are updated coherently within a single iterative loop.

Outer-loop convergence is declared once the Nash equilibrium residual satisfies $\varepsilon_{DN} < \varepsilon_{\text{outer}} = 10^{-5}$ and the relative variations of both cost functionals fall below $\varepsilon_J = 10^{-4}$ thereby ensuring both strategic consistency and stabilization of the objective functions. To further enhance computational efficiency, each player's inner optimization is initialized using the optimal control obtained at the previous outer iteration-namely $\overline{\eta}_{Dh}^k$ for the Dirichlet player and $\overline{\eta}_{Nh}^k$ for the Neumann player. This warm-start strategy is fully consistent with the one-shot philosophy and significantly accelerates convergence in the later stages of the algorithm. The complete procedure is summarized in Algorithm 1, referred to as the Nash Game Alternating Algorithm.

Algorithm 1 Nash Game Alternating Algorithm

Initialize: $k \leftarrow 0$, initial state $(\overline{\eta}^0_{Dh}, \overline{\eta}^0_{Nh})$
while not converged **do**
  Step 1: Dirichlet Player Optimization
  Set $s \leftarrow 0$, $\varepsilon_D \leftarrow 1$, $\eta^{k+1,0}_{Dh} \leftarrow \overline{\eta}^k_{Dh}$
  while $\varepsilon_D > \varepsilon_{\text{inner}}$ **do**
    Solve state equation (42) and adjoint (44)
    Compute gradient: $d^s_D = -(S^i_{ND}\mu^i_{Dh} + \alpha\eta^{k+1,s}_{Dh})$
    Update: $\eta^{k+1,s+1}_{Dh} = \eta^{k+1,s}_{Dh} + \alpha_D d^s_D$
    Compute ε_D with (46)
    $s \leftarrow s + 1$
  end while
  $\overline{\eta}^{k+1}_{Dh} = \eta^{k+1,s}_{Dh}$, $J^{k+1}_D = H^{\delta,\alpha}_{Dh}(\overline{\eta}^{k+1}_{Dh}, \overline{\eta}^k_{Nh})$
  Step 2: Neumann Player Optimization
  Set $s \leftarrow 0$, $\varepsilon_N \leftarrow 1$, $\eta^{k+1,0}_{Nh} \leftarrow \overline{\eta}^k_{Nh}$
  while $\varepsilon_N > \varepsilon_{\text{inner}}$ **do**
    Solve state equation (43) and adjoint (45)
    Compute gradient: $d^s_N = -(S^i_{ND}\mu^i_{Nh} + \alpha\eta^{k+1,s}_{Nh})$
    Update: $\eta^{k+1,s+1}_{Nh} = \eta^{k+1,s}_{Nh} + \alpha_N d^s_N$
    Compute ε_N with (46).
    $s \leftarrow s + 1$
  end while
  $\overline{\eta}^{k+1}_{Nh} = \eta^{k+1,s}_{Nh}$, $J^{k+1}_N = H^{\delta,\alpha}_{Nh}(\overline{\eta}^{k+1}_{Dh}, \overline{\eta}^{k+1}_{Nh})$
  Step 3: Convergence Check
  Compute ε_{DN} with (47)
  $\Delta J_D = |(J^{k+1}_D - J^k_D)/J^k_D|$, $\Delta J_N = |(J^{k+1}_N - J^k_N)/J^k_N|$
  if $\varepsilon_{DN} < \varepsilon_{\text{outer}}$ and $\Delta J_D < \varepsilon_J$ and $\Delta J_N < \varepsilon_J$ **then**
    converged $\leftarrow$ **true**
  end if
  $k \leftarrow k + 1$
end while

5 Numerical Results

We validate our Nash-game approach for Cauchy problems through comprehensive numerical experiments on two canonical domains: a full annulus and its upper semi-annular counterpart. These geometries present progressively challenging scenarios—from smooth boundaries to configurations with mixed boundary conditions—allowing us to assess method robustness across various boundary condition types. We generates exact Cauchy data on both domains using the following harmonic function:

$$ue(x, y) = \sin(0.5\pi y)\cosh(0.5\pi x).$$

To evaluate performance under realistic conditions, we introduce multiplicative white noise:

$$T^\delta = (1 + \delta\omega)T, \quad \phi^\delta = (1 + \delta\omega)\phi,$$

where δ represents the noise level and $\omega \sim \mathcal{N}(0,1)$ restricted to $[-1,1]$. The first domain is a full annulus centered at $(0,0)$ with outer radius $R_1 = 1$ and inner radius $R_2 = 0.75$:

$$\begin{aligned}\Gamma_i &= \{(x,y) \mid x^2 + y^2 = R_2\} \quad \text{(inaccessible)},\\ \Gamma_c &= \{(x,y) \mid x^2 + y^2 = R_1\} \quad \text{(Cauchy data)},\end{aligned}$$

with $\Gamma_0 = \emptyset$ in the general formulation (1). The control variables (η_D, η_N) belong to $(H^{1/2}(\Gamma_i))^2$. The second domain is the upper semi-annulus of the same dimensions:

$$\begin{aligned}\Gamma_0 &= \{(x,0) \mid R_2 \le |x| \le R_1\} \quad \text{(homogeneous Dirichlet)},\\ \Gamma_i &= \{(x,y) \mid x^2 + y^2 = R_2,\ y \ge 0\} \quad \text{(inaccessible)},\\ \Gamma_c &= \{(x,y) \mid x^2 + y^2 = R_1,\ y \ge 0\} \quad \text{(Cauchy data)}.\end{aligned}$$

Here, the control variables (η_D, η_N) belong to $(\widehat{H}^{\frac{1}{2}}(\Gamma_i))^2$, accounting for the homogeneous Dirichlet condition on the adjacent boundary Γ_0.
The first configuration is used as a smooth reference benchmark, since no Dirichlet–Neumann transition point is present. In contrast, the second configuration is designed to test the method in a more delicate setting involving Dirichlet–Neumann transition points at the junctions between Γ_0 and Γ_i. According to the regularity theory for elliptic problems in nonsmooth domains with mixed boundary conditions [21, 26, 39], such transition points may generate local singular components and reduce the effective Sobolev regularity of the solution. This second configuration is therefore used to assess the robustness of the Nash-game reconstruction in a reduced-regularity regime.
All computations employ GETFEM++ [43] with unstructured meshes, examining method performance across noise levels, regularization parameters, coupling coefficients, and mesh refinements.

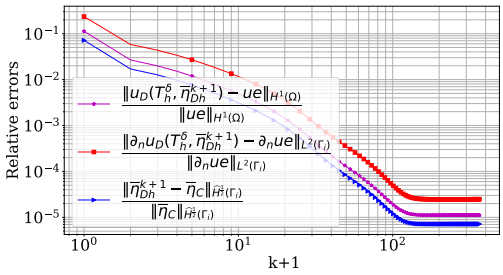
5.1 An Annular Domain

5.1.1 Algorithm Performance with Exact Data

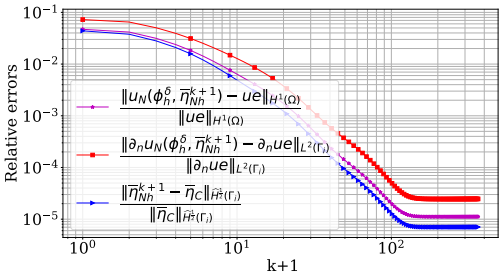
We analyze the convergence behavior of Algorithm 1 by depicting the evolution of the cost functionals $H_D^{\gamma,\delta,\alpha}(\overline{\eta}_{Dh}^k)$ and $H_N^{\gamma,\delta,\alpha}(\overline{\eta}_{Nh}^k)$ for both players, alongside the relative errors between the exact solution ue and the approximate solutions $u_D(T_h^\delta, \overline{\eta}_{Dh}^k)$ and $u_N(\phi_h^\delta, \overline{\eta}_{Nh}^k)$, as shown in Figure 2.

Due to the high number of degrees of freedom, the algorithm requires 365 iterations to meet the strict Nash equilibrium convergence tolerance. However, the convergence profile indicates that approximately 120 iterations suffice to capture the essential solution accuracy, suggesting significant computational savings are possible by relaxing the outer tolerance. Beyond this point, the players cannot significantly improve their strategies, confirming that a Nash equilibrium and a best-response compromise have been effectively attained.

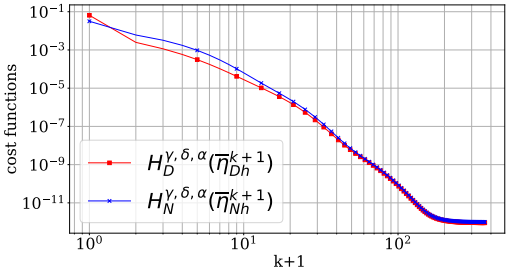
The method achieves high accuracy across all relevant norms. The relative error in $\mathbb{H}^1(\Omega)$ is approximately 1.1×10^{-5} for both solutions. On the inaccessible boundary Γ_i, the error is 2.5×10^{-5} in $\mathbb{L}^2(\Gamma_i)$ for the normal derivative and 7×10^{-6} in $\widehat{H}^{\frac{1}{2}}(\Gamma_i)$ for the trace. The total error is dominated by the $\mathbb{L}^2(\Gamma_i)$ norm of the normal derivative. These results demonstrate the efficiency and robustness of our approach for this noise-free benchmark.



(a) Relative error for the Dirichlet player

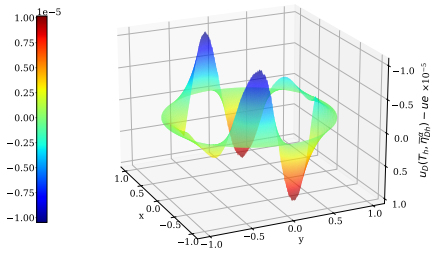


(b) Relative error for the Neumann player

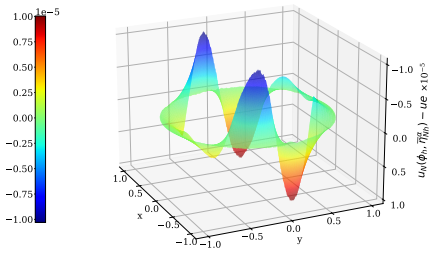


(c) Evolution of cost functionals

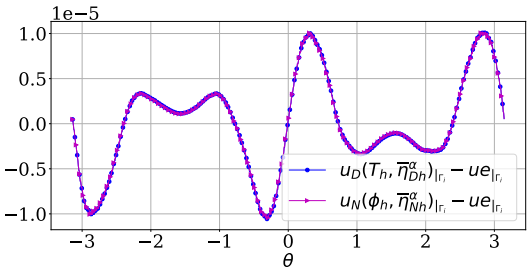
Figure 2: Convergence history for the noise-free case ($\delta = 0$), with $h = 0.005$ and $\alpha = 10^{-6}$. The top row shows the relative errors for (a) the Dirichlet player and (b) the Neumann player. The bottom plot (c) tracks the decay of the respective cost functionals.



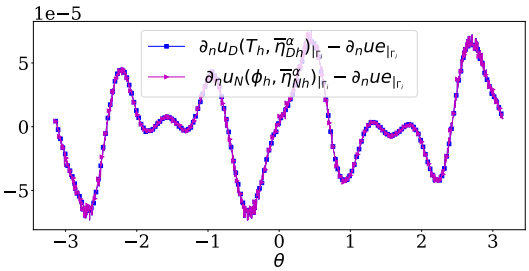
(a) Domain error: Dirichlet formulation



(b) Domain error: Neumann formulation



(c) Boundary trace error: $(u_h - u_e)|_{\Gamma_i}$



(d) Flux error: $(\partial_n u_h - \partial_n u_e)|_{\Gamma_i}$

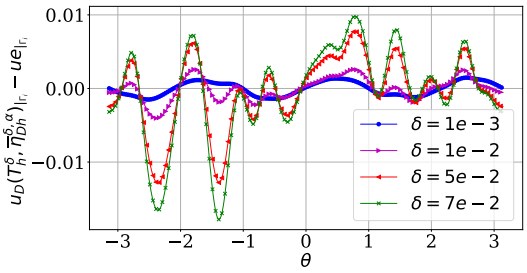
Figure 3: Comprehensive error analysis for the reconstructed solution ($h = 0.005$, $\alpha = 10^{-6}$). Top row: Spatial distribution of pointwise errors $|u_h - u_e|$ throughout the domain for (a) Dirichlet and (b) Neumann formulations. Bottom row: Pointwise reconstruction errors on the inaccessible boundary Γ_i for (c) the Dirichlet trace and (d) the Neumann flux.

The comprehensive error analysis in Figure 3 demonstrates the method's effectiveness across both domain reconstruction and boundary data recovery. The top row shows excellent agreement between the exact and reconstructed solutions throughout the annular domain, with minimal and uniformly distributed errors for both formulations. The bottom row quantifies the accuracy of boundary reconstruction on Γ_i, confirming that the method successfully recovers the complete Cauchy data with consistent precision along the entire interface. These results collectively validate the stability and robustness of our approach.

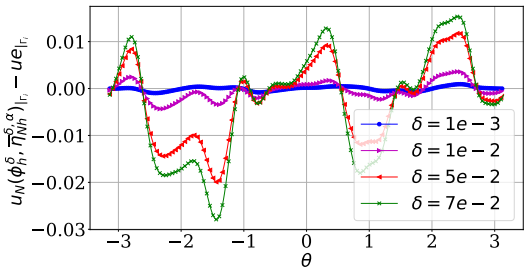
5.1.2 Sensitivity to Perturbed Cauchy Data

We now examine the sensitivity of the proposed method to perturbations in the Cauchy data. Figure 4 shows the trace and normal derivative errors on the inaccessible boundary Γ_i as the noise level δ varies, with $h = 0.005$, $\alpha = \delta/10$, and $\gamma = 0.5$. Specifically, we plot the differences between the exact solution u_e and the reconstructed solutions $u_D(T_h^{\delta}, \overline{\eta}_{Dh}^{\delta,\alpha})$ and $u_N(\phi_h^{\delta}, \overline{\eta}_{Nh}^{\delta,\alpha})$.

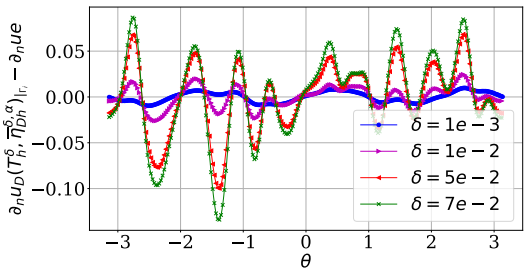
Despite significant noise in the over-specified data on Γ_c, our Nash game method maintains accurate reconstructions on Γ_i. These results demonstrate the robustness of the approach when the regularization parameter α is properly scaled with the noise level δ.



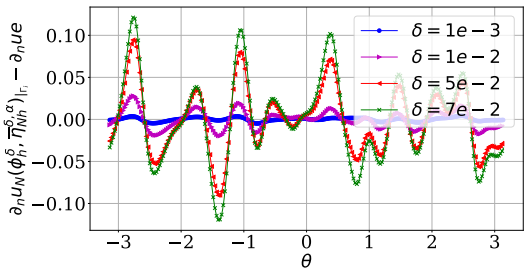
(a) Trace error: $u_D - u_e$ on Γ_i



(b) Trace error: $u_N - u_e$ on Γ_i



(c) Normal derivative error: $\partial_n u_D - \partial_n u_e$

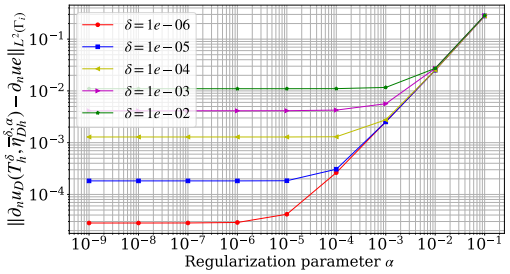


(d) Normal derivative error: $\partial_n u_N - \partial_n u_e$

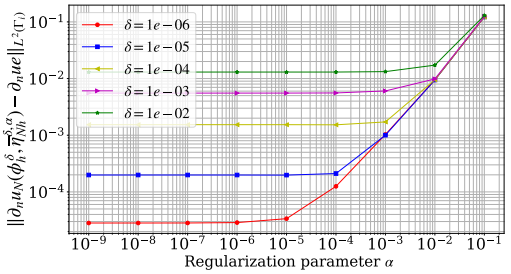
Figure 4: Sensitivity analysis: reconstruction errors on Γ_i for varying noise levels δ ($h = 0.005$, $\alpha = \delta/10$, $\gamma = 0.5$). Top row: trace errors for (a) Dirichlet and (b) Neumann formulations. Bottom row: normal derivative errors for (c) Dirichlet and (d) Neumann formulations.

5.1.3 Parameter Analysis and Convergence Rates

We investigate the influence of key algorithmic parameters on reconstruction accuracy and computational performance. First, the regularization parameter α is analyzed by examining the L^2-relative error between the reconstructed normal derivatives ($\partial_n u_D$ or $\partial_n u_N$) and the exact normal derivative $\partial_n u_e$ on Γ_i. As shown in Figure 5, both formulations achieve minimal error when $\alpha \leq \delta/10$, validating the optimal scaling $\alpha \sim \delta$. For small α, the Nash-game strategy converges reliably, demonstrating the robustness of our stopping criterion.



(a) Dirichlet formulation

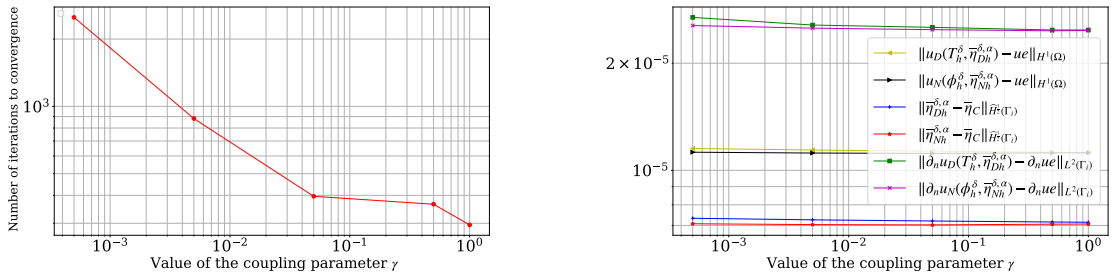


(b) Neumann formulation

Figure 5: Influence of regularization parameter α on L^2-relative error of normal derivative reconstruction ($h = 0.005$, $\gamma = 0.5$). Optimal accuracy is achieved when $\alpha \leq \delta/10$.

Next, the coupling parameter γ's effect is examined in Figure 6. Subfigure 6(a) shows that the

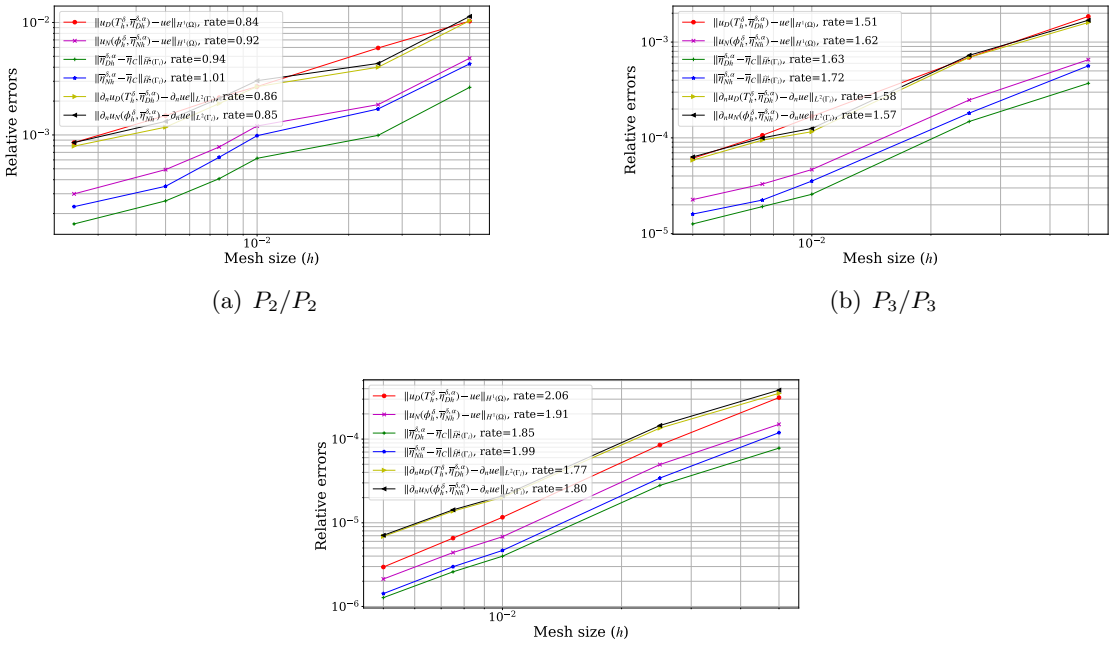
iteration count decreases with increasing γ until a stability threshold is reached. Subfigure 6(b) reveals that reconstruction errors remain essentially constant within the stable regime, indicating that γ primarily accelerates convergence without degrading accuracy. Moderate values of γ thus offer an optimal balance between speed and stability.



(a) Iteration count vs. γ (b) Relative errors vs. γ

Figure 6: Effect of coupling parameter γ on convergence speed and accuracy ($\delta = \alpha = 10^{-6}$, $h = 0.005$). Left: iteration count decreases with γ until divergence. Right: reconstruction errors remain stable across γ.

Finally, to numerically validate the a priori error estimate of Proposition 10, Figure 7 presents convergence rates for finite element pairs P_k/P_k ($k = 2, 3, 4$) with $\delta = \alpha/10 = h^{2k/3}$. Both formulations exhibit super-optimal convergence rates significantly exceeding the theoretical $k/3$ rate, demonstrating the efficiency of our numerical implementation.



(a) P_2/P_2 (b) P_3/P_3

(c) P_4/P_4

Figure 7: Convergence rates for P_k/P_k finite elements ($k = 2, 3, 4$) with $\delta = \alpha/10 = h^{2k/3}$. Observed rates are super-optimal and exceed theoretical predictions.

Our analysis confirms that (1) α should scale with δ for optimal accuracy, (2) γ effectively accelerates convergence without compromising reconstruction quality, and (3) the method achieves super-optimal convergence rates across polynomial orders, validating both algorithmic robustness and numerical efficiency.

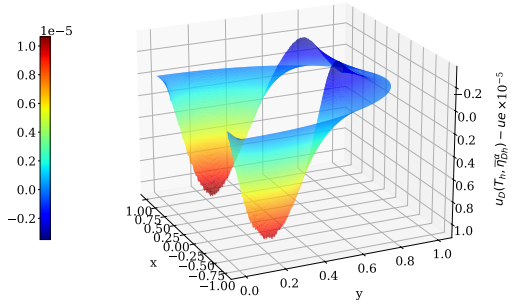
5.2 Upper Half-Annular Domain

We now consider the second test case on the upper half-annulus. In this configuration, the straight boundary segment Γ_0 meets the accessible and inaccessible parts of the boundary at Dirichlet–Neumann transition points. Such junctions are known to generate reduced-regularity effects for elliptic problems with mixed boundary conditions; see, for instance, [21, 26, 39]. In particular, near a Dirichlet–Neumann transition point, the local behavior of the solution may contain singular components whose Sobolev regularity is comparable to that of a function belonging only to

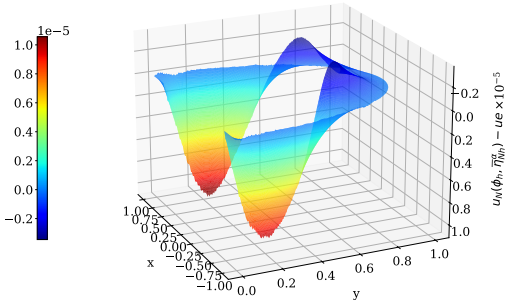
$$H^{2-\varepsilon}(\Omega), \qquad \varepsilon > 0.$$

This reduced-regularity effect is important for the subsequent interpretation of the numerical results, since it may limit the accuracy of the reconstruction and the convergence rates observed under mesh refinement. In the present test, the exact Cauchy data are generated from the same manufactured solution used in the previous configuration. Nevertheless, the upper half-annular geometry is designed to assess the sensitivity of the Nash-game reconstruction in the presence of Dirichlet–Neumann transition points. Even when the manufactured exact solution is smooth, the auxiliary boundary value problems solved during the iterative process involve approximate virtual controls on Γ_i. These approximate traces may fail to satisfy the local compatibility conditions at the transition points, thereby activating local singular components and producing a numerical behavior similar to that of a reduced-regularity problem.

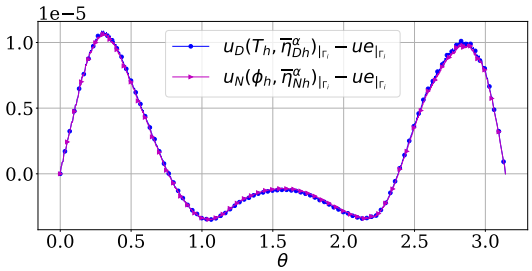
Beginning with exact noise-free Cauchy data ($\delta = 0$), and using $h = 0.005$, $\alpha = 10^{-6}$, and $\gamma = 0.5$, the reconstruction results are shown in Figures 8, 9, and 10. Figure 8 presents a comprehensive error analysis, including the pointwise reconstruction errors in the domain (8(a), 8(b)) and the corresponding trace and flux errors on the inaccessible boundary Γ_i (8(c), 8(d)). Compared with the full-annulus case, the error levels remain of the same order and the iteration counts reported in Figure 9 are very similar. This shows that the proposed Nash-game strategy remains stable in a configuration involving mixed boundary conditions and Dirichlet–Neumann transition points.
However, this observation should be interpreted carefully. The comparable error levels do not mean that the transition points have no effect. Rather, they indicate that, for the present smooth compatible data, the singular components associated with the exact solution are weak or may vanish. During the iterative process, however, the reconstructed virtual controls are only approximate and may activate reduced-regularity effects near the transition points.



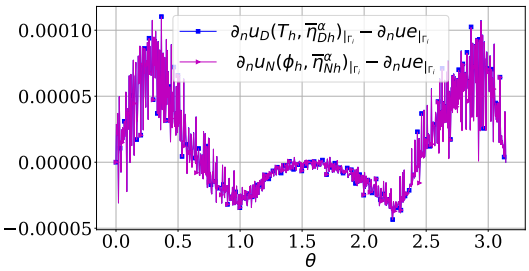
(a) Domain error: Dirichlet formulation



(b) Domain error: Neumann formulation

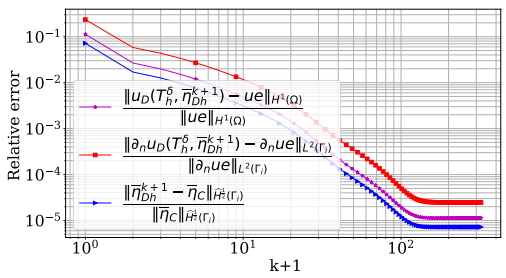


(c) Boundary trace error: $(u_h - u_e)|_{\Gamma_i}$

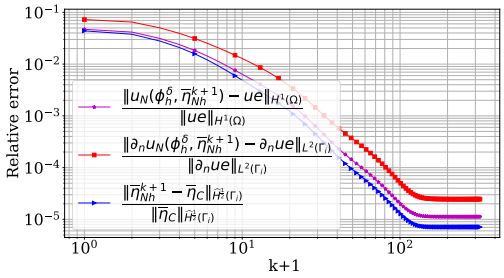


(d) Flux error: $(\partial_n u_h - \partial_n u_e)|_{\Gamma_i}$

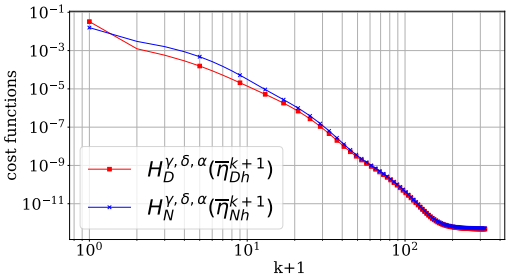
Figure 8: Comprehensive error analysis for the reconstructed solution on the upper half-annulus ($h = 0.005$, $\alpha = 10^{-6}$). Top row: Spatial distribution of pointwise errors $|u_h - u_e|$ throughout the domain for (a) Dirichlet and (b) Neumann formulations. Bottom row: Pointwise reconstruction errors on the inaccessible boundary Γ_i for (c) the Dirichlet trace and (d) the Neumann flux.



(a) Relative errors for the Dirichlet player

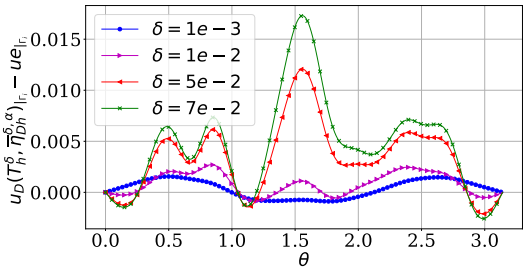


(b) Relative errors for the Neumann player

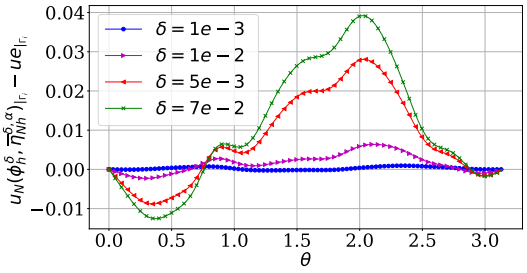


(c) Evolution of cost functionals H_D and H_N

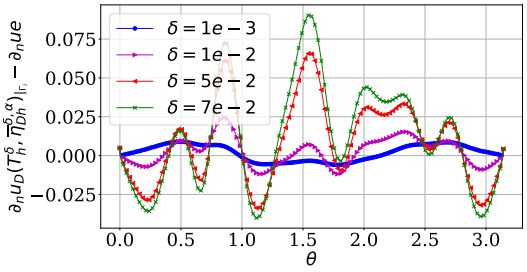
Figure 9: Convergence history for the noise-free upper half-annulus case ($\delta = 0$, $h = 0.005$, $\alpha = 10^{-6}$). Top: relative errors for each player's reconstruction. Bottom: decay of the respective cost functionals toward the Nash equilibrium.



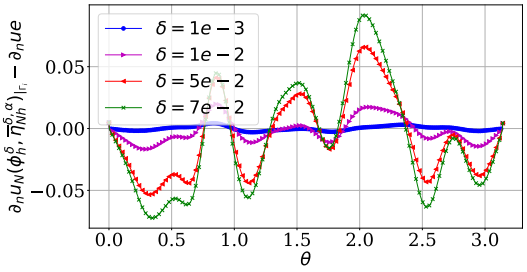
(a) Trace error $|u_D - u_e|$ on Γ_i for varying δ



(b) Trace error $|u_N - u_e|$ on Γ_i for varying δ



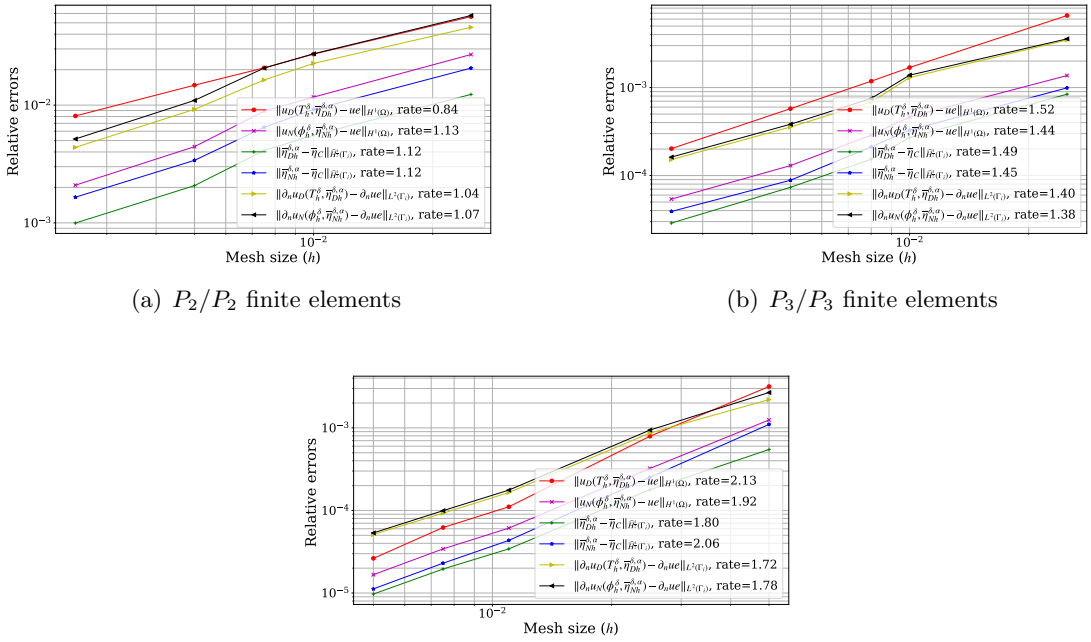
(c) Flux error $|\partial_n u_D - \partial_n u_e|$ on Γ_i for varying δ



(d) Flux error $|\partial_n u_N - \partial_n u_e|$ on Γ_i for varying δ

Figure 10: Sensitivity to noise: boundary reconstruction errors on Γ_i as the noise level δ increases ($h = 0.005$, $\alpha = \delta/10$, $\gamma = 0.5$). Top: Dirichlet trace errors. Bottom: Neumann flux errors.

We analyze the impact of data noise on the reconstruction along the inaccessible boundary Γ_i. Figure 10 shows how the trace and normal derivative errors on Γ_i vary with increasing noise level δ ($h = 0.005$, $\alpha = \delta/10$, $\gamma = 0.5$). Despite the local loss of regularity at the Dirichlet–Neumann junctions, the quality of the reconstructed boundary data remains comparable to that obtained for the full annular domain, demonstrating the robustness of our approach.



(a) P_2/P_2 finite elements

(b) P_3/P_3 finite elements

(c) P_4/P_4 finite elements

Figure 11: Convergence rates for different finite element pairs on the upper half-annulus ($\delta = \alpha/10 = h^{2k/3}$). Relative errors in $H^1(\Omega)$ and $L^2(\Gamma_i)$ norms versus mesh size h.

Finally, we assess convergence with respect to mesh refinement. Figure 11 shows the relative $H^1(\Omega)$-error of the reconstructed solution and the relative errors of the trace and normal derivative on Γ_i as functions of the mesh size h, for both the Dirichlet and Neumann formulations. Due to the Dirichlet–Neumann transition points, the numerical behavior is expected to be influenced by reduced-regularity effects. In view of the singular expansion theory for elliptic mixed boundary value problems [26, 21], such configurations may behave as if the relevant solution components belonged only to $H^{2-\varepsilon}(\Omega)$, for some $\varepsilon > 0$.
Accordingly, the theoretical estimate should be interpreted as a worst-case bound associated with limited regularity. If the effective regularity is close to $H^{2-\varepsilon}(\Omega)$, then the rate guaranteed by the estimate is lower than in the fully smooth case. The observed convergence rates in Figure 11 are higher than this minimal prediction and are close to those obtained in the full annulus. This should not be interpreted as a contradiction: the theoretical bound is not necessarily sharp, and the singular coefficients associated with the manufactured compatible data may be small or vanish. The results therefore show that the Nash-game formulation remains stable and accurate even in a geometry where Dirichlet–Neumann transition points may induce reduced-regularity effects.

Conclusion

In this paper, we introduced a Nash-game formulation for the Cauchy data completion problem associated with Laplace's equation. The missing boundary data on the inaccessible part of the boundary are represented by two independent virtual Dirichlet controls. These controls define two coupled players: one minimizes a Neumann gap functional, while the other minimizes a Dirichlet gap functional. The coupling between the two players enforces consistency of the reconstructed boundary information and leads to a non-cooperative game formulation of the data completion problem.

A rigorous analysis was carried out in energy trace spaces. We proved the existence and uniqueness of the Nash equilibrium and showed that, for compatible exact Cauchy data, this equilibrium coincides with the missing trace of the exact harmonic solution. This establishes the consistency of the game-theoretic formulation with the original Cauchy problem.

For noisy measurements, Tikhonov regularization was incorporated into both players' cost functionals. The main theoretical contribution of the paper is the derivation of explicit stability and error bound estimates for the regularized Nash equilibrium. These estimates quantify the dependence of the reconstruction error on the noise level δ, the regularization parameter α, and the coupling parameter γ. In particular, the analysis is valid in a practical finite-noise regime, where α remains in a fixed admissible interval $[\varepsilon, M]$, with $\varepsilon > 0$. Therefore, the estimates do not aim, by themselves, to prove asymptotic convergence as $\alpha \to 0$, but rather to provide robust error bounds for nonzero noise levels and admissible positive regularization parameters.

This point is essential in comparison with classical Tikhonov regularization theory. In the classical asymptotic framework, convergence rates are usually obtained under source-type or spectral regularity assumptions on the exact solution. By contrast, the present estimates are established under the baseline assumption that the missing trace belongs to $\widehat{H}^{1/2}(\Gamma_i)$, and do not require additional spectral source conditions. Thus, the proposed analysis complements classical Tikhonov theory by addressing the finite-noise regime encountered in practical computations.

A conforming finite element discretization of the Nash-game formulation was then developed. The numerical solution was computed by an alternating minimization algorithm combined with adjoint-based gradient evaluations. Numerical experiments on annular and half-annular geometries confirm the accuracy and robustness of the method. The results show that the proposed formulation remains stable for nonzero noise levels and provides accurate reconstructions of the interior solution, the missing boundary trace, and the normal derivative on the inaccessible boundary.

Several perspectives follow from this work. First, the selection of the regularization parameter α and the coupling parameter γ could be further investigated through discrepancy principles, adaptive strategies, or data-driven rules. Second, the analysis could be extended to more general elliptic systems, including linear elasticity and anisotropic models. Third, the proposed game-theoretic framework could be combined with uncertainty quantification or Bayesian approaches in order to provide confidence measures for the reconstructed boundary data. Finally, the development of adaptive finite element methods and the validation on experimental data constitute important directions for future research.

Acknowledgements

The second and third authors gratefully acknowledge the financial support received from the Tunisian Ministry of Higher Education.

Conflict of Interest

The authors declare that they have no conflict of interest.

Data Availability Statement

No datasets were generated or analyzed during the current study.

References

[1] Abid, C., Boukari, Y., Delvare, F.: Fading regularization method for the Helmholtz equation using boundary integral equations. Journal of Computational and Applied Mathematics **472**, 116818 (2026). URL https://doi.org/10.1016/j.cam.2025.116818

[2] Amdouni, S., Ben Abda, A.: The Cauchy problem for Laplace's equation via a modified conjugate gradient method and energy space approaches. Mathematical Methods in the Applied Sciences **46**(4), 3560–3582 (2023). DOI 10.1002/mma.8710. URL https://doi.org/10.1002/mma.8710

[3] Amdouni, S., Samaali, A.: Robustness analysis of an energy space method for solving a data completion problem in linear elasticity: S. amdouni, a. samaali. Journal of Optimization Theory and Applications **209**(1), 25 (2026)

[4] Andrieux, S., Baranger, T.N., Ben Abda, A.: Solving Cauchy problems by minimizing an energy-like functional. Inverse Problems **22**(1), 115–133 (2006). URL https://doi.org/10.1088/0266-5611/22/1/008

[5] Andrieux, S., Ben Abda, A., Baranger, T.N.: Data completion via an energy error functional. Comptes Rendus Mécanique **333**(2), 171–177 (2005). URL https://doi.org/10.1016/j.crme.2004.12.003

[6] Attouch, H., Bolte, J., Redont, P., Soubeyran, A.: Alternating proximal algorithms for weakly coupled convex minimization problems: Applications to dynamical games and PDEs. Journal of Convex Analysis **15**(3), 485–506 (2008). URL https://doi.org/10.5802/afst.541

[7] Aumann, R.J., Peleg, B.: Von Neumann–Morgenstern solutions to cooperative games without side payments. Bulletin of the American Mathematical Society **66**(3), 173–179 (1960). URL https://www.ams.org/journals/bull/1960-66-03/S0002-9904-1960-10418-1/

[8] Azaïez, M., Belgacem, F.B., Du, D.T., Jelassi, F.: A finite element model for the data completion problem: analysis and assessment. Inverse Problems in Science and Engineering **19**(8), 1063–1086 (2011). URL https://doi.org/10.1080/17415977.2011.587515

[9] Ben Abda, A., Jaïem, E., Mejri, B.: Constitutive law misfit functional: A guided tour (2021). URL https://hal.science/hal-03168249. Working paper

[10] Ben Belgacem, F.: Why is the Cauchy problem severely ill-posed? Inverse Problems **23**(2), 823–836 (2007). URL https://doi.org/10.1088/0266-5611/23/2/020

[11] Ben Belgacem, F., Girault, V., Jelassi, F.: Full discretization of Cauchy's problem by Lavrentiev–finite element method. SIAM Journal on Numerical Analysis **60**(2), 558–584 (2022). DOI 10.1137/21M1401310. URL https://doi.org/10.1137/21M1401310

[12] Bonazzoli, M., Haddar, H., Vu, T.A.: On the convergence analysis of one-shot inversion methods. SIAM Journal on Applied Mathematics **84**(6), 2440–2475 (2024). URL https://doi.org/10.1137/23M1585866

[13] Boukraa, M.A., Amdouni, S., Delvare, F.: Fading regularization fem algorithms for the Cauchy problem associated with the two-dimensional biharmonic equation. Mathematical Methods in the Applied Sciences **46**(2), 2389–2412 (2023). URL https://doi.org/10.1002/mma.8651

[14] Brühl, M., Hanke, M., Pidcock, M.: Crack detection using electrostatic measurements. ESAIM: Modélisation mathématique et analyse numérique **35**(3), 595–605 (2001). URL https://www.numdam.org/item/M2AN_2001__35_3_595_0/

[15] Chamekh, R., Habbal, A., Kallel, M., Zemzemi, N.: A Nash game algorithm for the solution of coupled conductivity identification and data completion in cardiac electrophysiology. Mathematical Modelling of Natural Phenomena **14**(2), 201 (2019). URL https://doi.org/10.1051/mmnp/2018059

[16] Chen, H.Q., Glowinski, R., Périaux, J.: A domain decomposition/nash equilibrium methodology for the solution of direct and inverse problems in fluid dynamics with evolutionary algorithms. In: U. Langer, M. Discacciati, D.E. Keyes, O.B. Widlund, W. Zulehner (eds.) Domain Decomposition Methods in Science and Engineering XVII, pp. 21–32. Springer Berlin Heidelberg, Berlin, Heidelberg (2008). DOI 10.1007/978-3-540-75199-1_2

[17] Ciarlet, P.G.: The Finite Element Method for Elliptic Problems, *Classics in Applied Mathematics*, vol. 40. Society for Industrial and Applied Mathematics (SIAM), Philadelphia, PA (2002). URL https://doi.org/10.1137/1.9780898719208

[18] Cimetière, A., Delvare, F., Jaoua, M., Pons, F.: Solution of the Cauchy problem using iterated Tikhonov regularization. Inverse Problems **17**(3), 553–570 (2001). URL https://doi.org/10.1088/0266-5611/17/3/313

[19] Cîmpean, I., Grecu, A., Marin, L.: Numerical spectral analysis of cauchy-type inverse problems: A probabilistic approach (2025). URL https://arxiv.org/abs/2409.03686

[20] Dashti, M., Stuart, A.M.: The Bayesian Approach to Inverse Problems, pp. 311–428. Springer International Publishing, Cham (2017). URL https://doi.org/10.1007/978-3-319-12385-1_7

[21] Dauge, M.: Elliptic Boundary Value Problems on Corner Domains: Smoothness and Asymptotics of Solutions. Springer, Berlin, Heidelberg (1988). DOI 10.1007/BFb0086682

[22] Delvare, F., Cimetière, A., Pons, F.: An iterative boundary element method for Cauchy inverse problems. Computational Mechanics **28**(3), 291–302 (2002). URL https://doi.org/10.1007/s00466-001-0292-9

[23] Ern, A., Guermond, J.L.: Theory and Practice of Finite Elements, *Applied Mathematical Sciences*, vol. 159. Springer-Verlag, New York (2004). URL https://doi.org/10.1007/978-1-4757-4355-5

[24] Fursikov, A.V.: Optimal Control of Distributed Systems: Theory and Applications, *Translations of Mathematical Monographs*, vol. 187. American Mathematical Society, Providence, RI (1999)

[25] Gong, R., Wang, M., Huang, Q., Zhang, Y.: A ccbm-based generalized gkb iterative regularization algorithm for inverse cauchy problems. Journal of Computational and Applied Mathematics **432**, 115,282 (2023). URL https://www.sciencedirect.com/science/article/pii/S0377042723002261

[26] Grisvard, P.: Elliptic Problems in Nonsmooth Domains. Pitman, Boston (1985)

[27] Habbal, A., Kallel, M.: Neumann–Dirichlet Nash strategies for the solution of elliptic Cauchy problems. SIAM Journal on Control and Optimization **51**(5), 4066–4083 (2013). URL https://doi.org/10.1137/120869808

[28] Hadamard, J.: Lectures on Cauchy's Problem in Linear Partial Differential Equations. Yale University Press, New Haven (1923)

[29] Hao, D.N., Lesnic, D.: The Cauchy problem for Laplace's equation via the conjugate gradient method. IMA Journal of Applied Mathematics **65**(2), 199–217 (2000). URL https://doi.org/10.1093/imamat/65.2.199

[30] Jin, B., Zou, J.: A bayesian inference approach to the ill-posed Cauchy problem of steady-state heat conduction. International Journal for Numerical Methods in Engineering **76**(4), 521–544 (2008). URL https://doi.org/10.1002/nme.2350

[31] Kallel, M., Moakher, M., Theljani, A.: The Cauchy problem for a nonlinear elliptic equation: Nash-game approach and application to image inpainting. Inverse Problems and Imaging **9**(3), 853–874 (2015). URL https://doi.org/10.3934/ipi.2015.9.853

[32] Klapper, I., Szyld, D.B., Yu, X., Zengler, K., Zhang, T., Zúñiga, C.: A domain decomposition method for solution of a PDE-constrained generalized Nash equilibrium model of biofilm community metabolism. SIAM Journal on Applied Mathematics **84**(1), 97–113 (2024). URL https://doi.org/10.1137/22M1511023

[33] Kohn, R.V., Kohn, M.: Determining conductivity by boundary measurements ii. interior results. Communications on Pure and Applied Mathematics **38**(5), 643–667 (1985). URL https://doi.org/10.1002/cpa.3160380513

[34] Koshev, N., Yavich, N., Malovichko, M., Skidchenko, E., Fedorov, M.: FEM-based Scalp-to-Cortex EEG data mapping via the solution of the Cauchy problem. Journal of Inverse and Ill-posed Problems **28**(4), 517–532 (2020). URL https://doi.org/10.1515/jiip-2019-0065

[35] Kozlov, V.A., Maz'ya, V.G., Fomin, A.V.: An iterative method for solving the Cauchy problem for elliptic equations. Computational Mathematics and Mathematical Physics **31**(1), 45–52 (1991)

[36] Lions, J.L., Magenes, E.: Non-Homogeneous Boundary Value Problems and Applications. Vol. I, *Die Grundlehren der mathematischen Wissenschaften*, vol. 181. Springer, Berlin, Heidelberg (1972). URL https://doi.org/10.1007/978-3-642-65161-8

[37] Marin, L.: Boundary element–minimal error method for the Cauchy problem associated with Helmholtz-type equations. Computational Mechanics **44**(2), 205–219 (2009). URL https://doi.org/10.1007/s00466-009-0368-5

[38] Nash, J.F.: Equilibrium points in n-person games. Proceedings of the National Academy of Sciences of the United States of America **36**(1), 48–49 (1950). URL https://doi.org/10.1073/pnas.36.1.48

[39] Nicaise, S.: About the Lamé system in a polygonal or a polyhedral domain and a coupled problem between the Lamé system and the plate equation. I : regularity of the solutions. Annali della Scuola Normale Superiore di Pisa - Classe di Scienze **Ser. 4, 19**(3), 327–361 (1992). URL https://www.numdam.org/item/ASNSP_1992_4_19_3_327_0/

[40] Ouni, M., Habbal, A., Kallel, M.: A Nash-game approach to joint data completion and location of small inclusions in Stokes flow. Revue Africaine de Recherche en Informatique et Mathématiques Appliquées **34**, 1–23 (2021). URL https://doi.org/10.46298/arima.6761

[41] Quarteroni, A., Valli, A.: Domain Decomposition Methods for Partial Differential Equations. Oxford University Press, Oxford (1999). URL https://doi.org/10.1093/oso/9780198501787.001.0001

[42] Ramos, A.M., Glowinski, R., Périaux, J.: Nash equilibria for the multiobjective control of linear partial differential equations. Journal of Optimization Theory and Applications **112**(3), 457–498 (2002). URL https://doi.org/10.1023/A:1017981514093

[43] Renard, Y., Poulios, K.: Getfem: Automated FE modeling of multiphysics problems based on a generic weak form language. ACM Transactions on Mathematical Software (TOMS) **47**(1), 1–31 (2020). URL https://doi.org/10.1145/3412849

[44] Roy, S., Pal, S.: A PINN-driven game-theoretic framework in limited data photoacoustic tomography. Inverse Problems **41**(2), 025005 (2025). URL https://doi.org/10.1088/1361-6420/ae1bcd

[45] Sayas, F.J., Brown, T.S., Hassell, M.E.: Variational Techniques for Elliptic Partial Differential Equations: Theoretical Tools and Advanced Applications. CRC Press, Boca Raton, FL (2019). URL https://doi.org/10.1201/9780429507069

[46] Scherzer, O., Grasmair, M., Grossauer, H., Haltmeier, M., Lenzen, F.: Variational Regularization Methods for the Solution of Inverse Problems, pp. 53–113. Springer New York, New York, NY (2009). URL https://doi.org/10.1007/978-0-387-69277-7_3

[47] Steinbach, O.: Numerical Approximation Methods for Elliptic Boundary Value Problems: Finite and Boundary Elements, *Springer Series in Computational Mathematics*, vol. 38. Springer, New York (2007). URL https://doi.org/10.1007/978-0-387-68805-3

[48] Tikhonov, A.N.: On the solution of ill-posed problems and the method of regularization. Doklady Akademii Nauk SSSR **151**, 501–504 (1963)

[49] Tikhonov, A.N., Arsenin, V.Y.: Solutions of Ill-Posed Problems. Scripta Series in Mathematics. V. H. Winston & Sons, Washington, DC; John Wiley & Sons, New York-Toronto-London (1977). Translated from the Russian, Preface by translation editor Fritz John

[50] Vu, T.A.: One-shot inversion methods and domain decomposition. Ph.D. thesis, Institut Polytechnique de Paris, Palaiseau, France (2024). URL https://theses.hal.science/tel-04667744v1

[51] Zayeni, H., Abda, A.B., Delvare, F., Khayat, F.: Fading regularization MFS algorithm for the Cauchy problem associated with the two-dimensional Stokes equations. Numerical Algorithms **94**(3), 1461–1488 (2023). URL https://doi.org/10.1007/s11075-023-01543-8